AN ABSTRACT OF THE THESIS OF

Judson Stillman Matthias for the M.S. in Civil Engineering
(Name) (Degree) (Major)

Date thesis is presented May 3, 1963

Title INVESTIGATION OF THE EFFECTS OF SKEWED CONTRACTION JOINTS ON CONCRETE ROADWAY SLABS

Abstract approved
(Major professor)

The effects on the internal flexural stress of a concrete pavement caused by axle loads crossing skewed contraction joints were studied.

The analytical solution was based on data from a model slab which was tested using SR 4 strain gages to record the strains caused by axle loads. An analytical evaluation of the skewed configuration was made using influence charts developed by Pickett and Ray for the solution of Westergaard's equations. Westergaard's equations, thus also the influence charts, determine the flexural stress caused in rigid pavement slabs by live loads.

The model slab was seven feet by two feet by two inches. Provisions were made for testing a skewed joint and a joint perpendicular to the center line by placing strain gages in pairs longitudinally and transversely at both edges, quarter points, and on the center line of each joint. The model was tested by placing a

simulated axle load at successive two inch intervals across each joint. This was done for the solid slab condition and also after the joints were cut by sawing.

An attempt was made to crack the joints completely by using hydraulic jacks but this was unsuccessful as the slab cracked in two places approximately eight inches from each joint.

There are indications that for the skewed joint, the transfer of load will reduce the impact stresses across the joints due to the fact that the wheels of an axle cross the joint at different times.

INVESTIGATION OF THE EFFECTS OF SKEWED CONTRACTION JOINTS ON CONCRETE ROADWAY SLABS

by

JUDSON STILLMAN MATTHIAS

A THESIS

submitted to

OREGON STATE UNIVERSITY

in partial fulfillment of
the requirements for the
degree of

MASTER OF SCIENCE

June 1963

APPROVED:

Redacted for privacy

Professor of Civil Engineering

In Charge of Major

Redacted for privacy

Head of Department of Civil Engineering

Redacted for privacy

Dean of Graduate School

Date thesis is presented May 3, 1963

Typed by Jolene Wuest

ACKNOWLEDGMENTS

I would like to acknowledge the assistance and guidance given to me in the preparation of this thesis.

I wish to thank Professor Martin P. Coopey who gave freely of his ideas, advice, and criticism from the inception of the idea, the construction of the slab, to the final proof reading of this thesis and did so much to make this project possible.

My thanks also go to Professor Glenn W. Holcomb for his timely advice and his encouragement and to Professor Thomas J. McClellan for his encouragement, advice, and criticism.

Judson Matthias

April, 1963.

TABLE OF CONTENTS

	Page
I. THE PURPOSE OF STUDY	1
II. METHOD OF STUDY	2
1. Basic Stresses and Influence Charts	2
2. Warping Stresses	12
3. Expansion and Contraction Stresses	13
III. MODEL TESTS	14
1. The Purpose	14
2. Model Development	14
3. Testing	23
IV. CONCLUSIONS	33
BIBLIOGRAPHY	43
APPENDICES	
A. DEFINITIONS	45
B. TEST DATA	46
1. Load Versus Strain Curves	47
2. Comparison Between Center Line Gages	67
3. Sample Computations	68
4. Strain Curves	77

LIST OF FIGURES

Figure		Page
1	Scale of Influence Chart	5
2	Differential Element	11
3	Location of Strain Gages	16
4	H-20 Highway Loading	18
5	H-20 Highway Loading Diagram	19
6	Brass Fork	22
7	Location of Loading Points	26
8	Loading Normal Joint	30
9	Loading Skewed Joint	30
10	Load versus Strain	47
11	Load versus Strain	48
12	Load versus Strain	49
13	Load versus Strain	50
14	Load versus Strain	51
15	Load versus Strain	52
16	Load versus Strain	53
17	Load versus Strain	54
18	Load versus Strain	55
19	Load versus Strain	56
20	Load versus Strain	57
21	Load versus Strain	58
22	Load versus Strain	59
23	Load versus Strain	60
24	Load versus Strain	61
25	Load versus Strain	62
26	Load versus Strain	63
27	Load versus Strain	64
28	Load versus Strain	65
29	Load versus Strain	66
30	Comparison Between Centerline Gages of Skewed (#6) and Normal (#18) Joints When Loaded on Centerline	67
31	Longitudinal Strain Curve	77
32	Longitudinal Strain Curve	78
33	Longitudinal Strain Curve	79
34	Longitudinal Strain Curve	80
35	Longitudinal Strain Curve	81
36	Longitudinal Strain Curve	82
37	Longitudinal Strain Curve Comparison	83
38	Longitudinal Strain Curve Comparison	84
39	Transverse Strain Curve	85

Figure		Page
40	Transverse Strain Curve	86
41	Transverse Strain Curve	87
42	Transverse Strain Curve	88
43	Transverse Strain Curve	89
44	Transverse Strain Curve Comparison	90
45	Transverse Strain Curve Comparison	91
46	Transverse Strain Curve	92

LIST OF TABLES

Table		Page
1	Skewed Joint Solid Slab	27
2	Normal Joint Solid Slab	28
3	Skewed Joint Cut Slab	29
4	Normal Joint Cut Slab	29
5	Stress Tables, Solid Slab	34
6	Stress Tables, Cut Slab	35
7	Difference Between Influence Chart Stress and Strain Gage Stress ----- Solid Slab	36
8	Difference Between Influence Chart Stress and Strain Gage Stress ----- Cut Slab	37
9	Stress Tables, Cracked Slab	40

LIST OF PLATES

Plates		Page
1	Influence Chart Used for Solid and Cut Analysis	7
2	Influence Chart Used for Cracked Analysis	8
3	Model Slab	15
4	Strain Wiring Under the Model	15
5	Skewed Joint	20
6	Joints and Load Positions	20
7	Strain Indicator and Switching Unit	24
8	End Clamps and Wiring Connections	24
9	Normal Joint and Transverse Crack	32
10	Loading Device with Weights	32

INVESTIGATION OF THE EFFECTS OF SKEWED CONTRACTION JOINTS ON CONCRETE ROADWAY SLABS

I. THE PURPOSE OF STUDY

Several state highway departments have begun, in recent years, to place contraction joints at an angle of less than ninety degrees with the center line of the pavement slab. This is being done to improve the riding characteristics of the highway by reducing the effect of the bump felt by the motorist as his vehicle passes over the joint. The bump caused by crossing the joint will be reduced if both wheels of an axle cross the joint at different times as would be the case when a skewed contraction joint is used. A skewed contraction joint is any joint that is not perpendicular to the longitudinal center line.

The purpose of this paper is to evaluate the stress conditions within the concrete pavement slab and to determine both if any significant changes in stresses occur and if any structural advantages are realized by utilizing skewed joints rather than the normal perpendicular contraction joints which are now in general use.

II. METHOD OF STUDY

1. Basic Stresses and Influence Charts

The definition of a concrete pavement slab must be made before any analysis of basic stresses can be undertaken because different methods are used to analyze flexible and rigid pavements. In this investigation rigid pavements were used. This means that, due to the relatively high rigidity and high modulus of elasticity, the pavement slab itself provides a major portion of the structural capacity of the pavement. Pavement includes both concrete slab and the subgrade. Minor variations in the subgrade do not have a great deal of influence on the structural capacity of the pavement because the major factor to be considered in the design of a rigid pavement is the structural strength of the concrete slab.

The stresses due to wheel loads on the slab may be found by using Westergaard's three methods of loading (16, p. 25). These methods consist of (1) load at the edge of the pavement, (2) an interior load, and (3) a corner load. The first method is applicable for the cracked condition of the slab. The second method is the applicable method for this investigation since only interior loads were used for the solid condition. The theory of elasticity as utilized by Westergaard provides an ordinary and a special theory for slabs with the

relative proportions of a highway pavement slab. The ordinary theory assumes that a straight line drawn through the slab perpendicular to the neutral axis remains straight and perpendicular to the neutral axis throughout the period of loading (16, p. 27). The third and special method covers the area around a point of concentrated load where the ordinary method breaks down. In this case, Hooke's law applies with geometrical continuity being maintained (16, p. 31). The formula that gives the critical stress for this condition is:

$$\sigma = \frac{0.316\ P}{h^2}\ (4 \log_{10} \left(\frac{l}{b}\right) + 1.069)$$

where $b = \sqrt{1.6a^2 = h^2} - 0.675\ h$ (18, p. 64).

Note: See Appendix A, page 45, for definition of all symbols used.

Because of the fact that the solution of Westergaard's equations requires a great deal of time and the analysis of a large number of variables, influence charts have been developed for the solution of the general equations (18, p. 65-66). The charts were constructed by solving the general equations developed by Westergaard to give the effects caused by various positions of load on any particular point, using the direction of travel as the reference axis.

An influence chart is similar to an influence line which is a curve, the ordinate to which at any point equals the value of some

particular function due to a load which acts at that point. Influence lines can be used to compute the value of that function for any loading condition. The influence charts developed by Pickett and Ray (9, p. 49) can be used to determine the effect at any point caused by a load or loads at any other point or points on the structure.

To use the influence charts it is necessary to construct an imprint of the contact area of the load. The form used by Pickett and Ray (18, p. 68) is oblong to conform to the imprint of a rubber tire on a pavement. The oblong configuration was not used for this analysis because a circular rubber disk was used to transfer the load from the circular pipe to the slab. Thus, the circular configuration was used. The imprint is constructed by drawing the contact area to scale. It is then traced on the chart using "l" as the scale of measurement. See Figure 1, page 5 for this. The number of blocks within the imprint area are counted and the moment equation:

$$M = \frac{Pl^2 N}{10,000}$$

is solved where:

$$l = \sqrt[4]{\frac{Eh^3}{12(1 - \mu^2)k}}$$

P = unit load (psi)

N = number of blocks

$$\frac{\text{length "l" shown on influence chart (inches)}}{\text{computed length of "l" (inches)}} = \text{scale}$$

For solid slab:

$$\frac{7.35 \text{ inches}}{29.7 \text{ inches}} = 0.247 \text{ inches}$$

0.247 inches on influence chart = one inch

For cut slab:

$$\frac{7.35 \text{ inches}}{25.2 \text{ inches}} = 0.292 \text{ inches}$$

0.292 inches on influence chart = one inch

Figure 1. Scale of Influence Chart

The stress can be found by solving $\frac{6M}{h^2}$, where h is the depth of the slab. Influence charts are available for several conditions of loading. Two were used in this investigation; interior and edge loading situations.

For this investigation, the interior load for moment chart was used for the solid state and the cut state analysis and the load in the vicinity of the edge for moment chart was used for the cracked slab analysis. See Plates 1 and 2, on pages 7 and 8, for photographs of the influence charts.

Value of l for solid slab and cracked slab analysis

$$l = \sqrt[4]{\frac{Eh^3}{12(1-\mu)k}}$$

$E = 3.5 \times 10^6$ psi

$h = 2$ inches

$\mu = 0.15$

$K = \frac{3 \text{ pounds}}{\text{inches}^3}$

$l = 29.7$ inches

Value of ℓ for cut slab

$h = 1.6$ inches

$\ell = 25.2$ inches

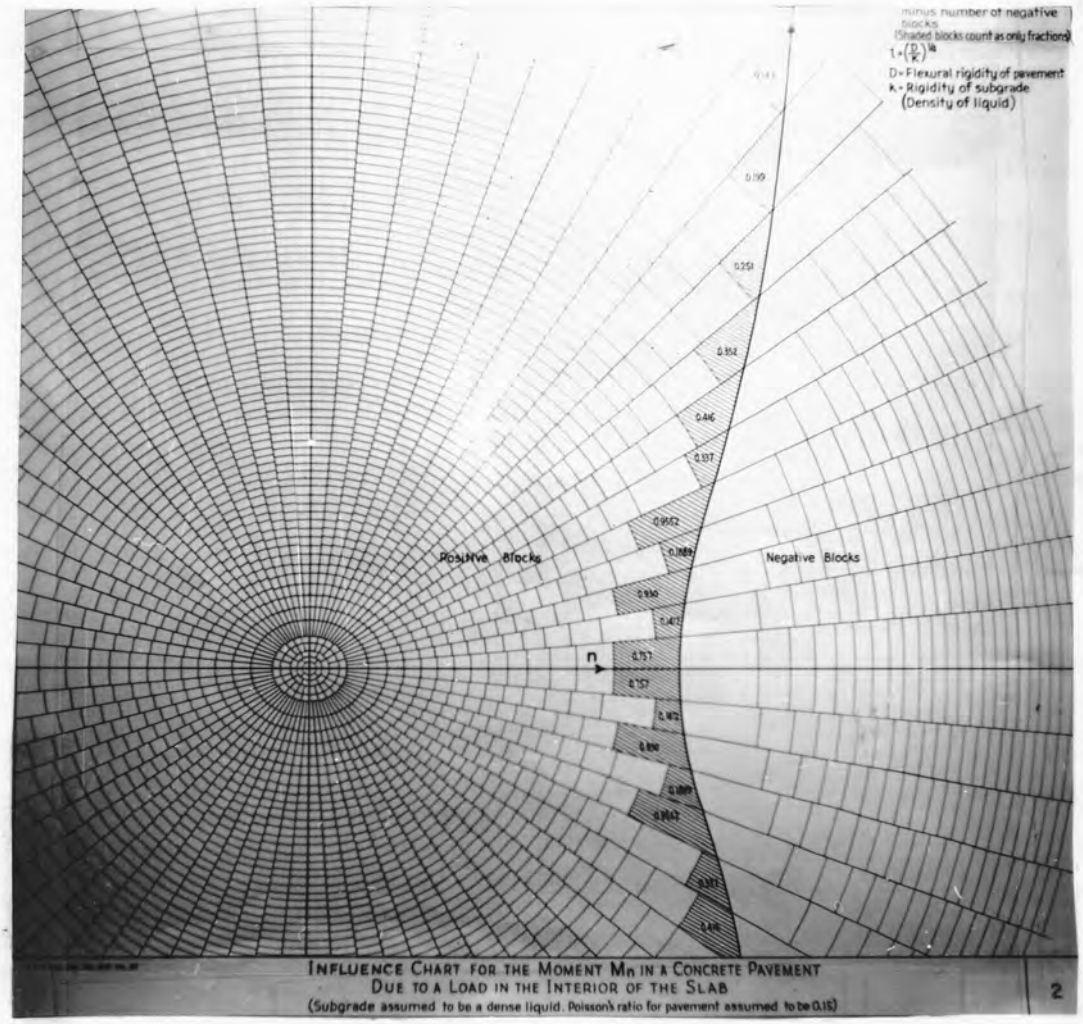

Plate 1. Influence Chart Used for Solid and Cut Analysis

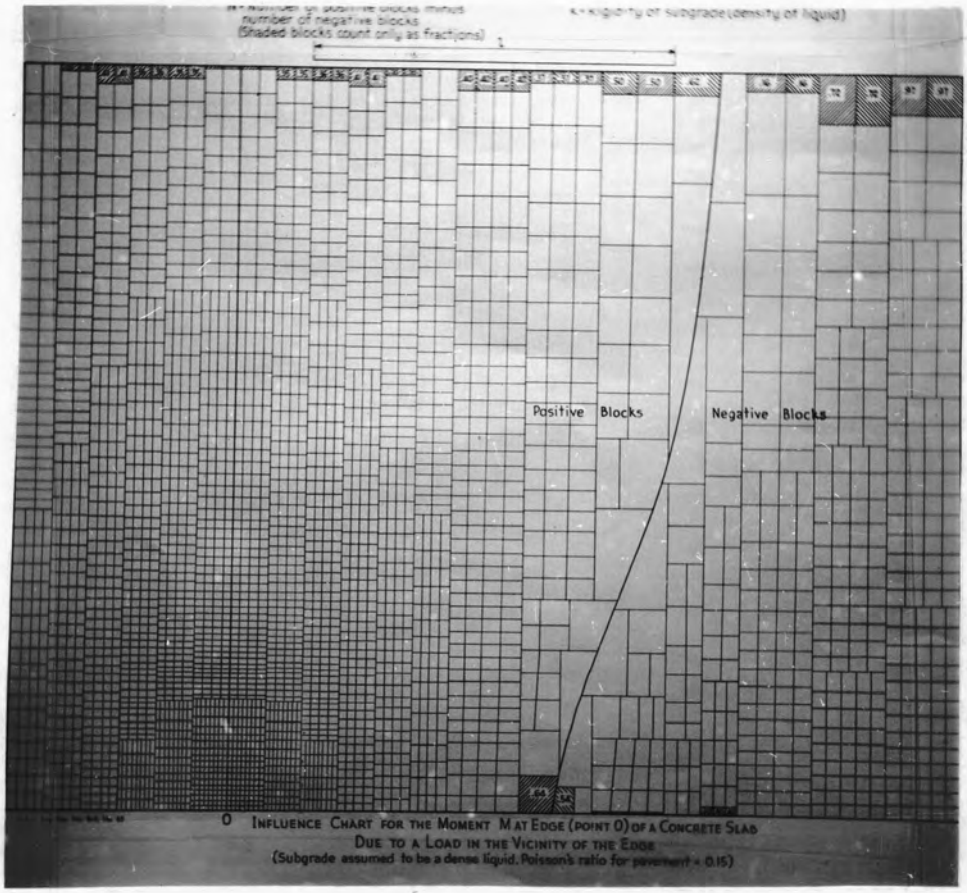

Plate 2. Influence Chart Used for Cracked Analysis

For this investigation, the assumption that the subgrade acts as a dense liquid was followed so that the conventional "k" or modulus of subgrade reaction could be used (18, p. 66). The modulus of subgrade reaction or "k" is the ratio of the load to the total of deflection of the material being investigated. In this case, the material is the foam rubber used as the subgrade.

The value of k used in this investigation was determined by test methods because no value could be found for the modulus of subgrade reaction for foam rubber. A box two feet square by one foot deep was filled with the same sand mixture that was used for the slab model subgrade. A piece of three inch thick foam rubber was placed in this box allowing for one quarter inch clearance with the sides of the box. A piece of three quarter inch plywood which had a circular hole five inches in diameter cut out of the center, was placed on the rubber. The square board was loaded so that the dead load of the slab on the concrete was duplicated and then the circular disk was loaded until the load reached one pound per square inch. Ames dials were used to measure the deflection of the disk. The dials were placed on opposite edges and the average of the readings was used as the deflection.

k - modulus of subgrade reaction

$$\text{area of plate} = \frac{\pi D^2}{4} = \frac{\pi \times 5^2}{4} = 19.61 \text{ inches}^2$$

dead load = 0.186 psi

load on plate = 0.186 x 19.61 = 3.64 pounds

weight of board = 6.75 pounds

area (less area of plate) = 22" x 21" = 462.00 - 19.61

= 442.39 inches^2

dead load = 442.39 x 0.186 = 82.21 pounds

weight that was necessary to add to the board = 82.21 - 6.75

= 75.46 pounds

$$k = \frac{P}{\Delta} = \frac{\text{unit load psi}}{\text{deflection (inches)}}$$

$$P = \frac{20 \text{ pounds}}{19.61 \text{ inches}^2} = 1.02 \text{ psi}$$

Δ = 690 x 0.0005 = 0.345 inches
679 x 0.0005 = 0.339 inches
694 x 0.0005 = 0.347 inches
698 x 0.0005 = 0.349 inches

average 0.345 inches

$$k = \frac{1.02 \text{ pounds per inch}^2}{0.345 \text{ inch}} = 2.95 \text{ or } \frac{3 \text{ pounds}}{\text{inches}^3}$$

The model test results were analyzed using Hooke's Law which states that the stress is proportional to the strain (13, p. 627).

Because two directional strains were recorded, a modification of Hooke's Law was used:

$$\epsilon_{\text{Longitudinal}} = \frac{\sigma_L}{E} - \mu \frac{\sigma_T}{E}$$

and

$$\epsilon_{\text{Transverse}} = \frac{\sigma_T}{E} - \mu \frac{\sigma_L}{E}$$

A modulus of elasticity (E) of 3.5×10^6 psi was assumed for this investigation. This is an average value for concrete and the value was used for all pertinent computations. Poisson's ratio (μ) for the concrete was assumed to be 0.15, a value selected as being an average value for concrete. Due to the light loads used, no recordings of vertical strains were made and are therefore not included. A biaxial stress condition was assumed.

A differential element of the slab would show the biaxial condition as:

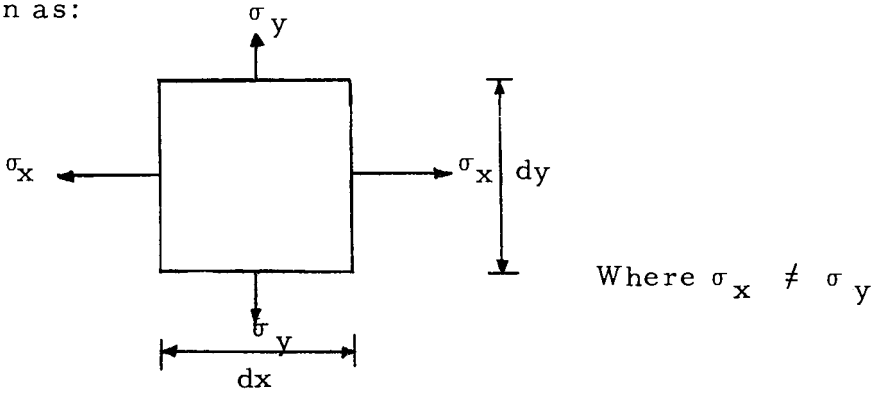

Figure 2. Differential Element.

The total biaxial stress at a point would be the shearing stress plus the tensile stress. Only the tensile stress could be found from the influence charts. Thus, only tensile stresses were used in the analysis. While the shearing stresses should not be ignored, only the tensile stresses could be measured due to the strain gage arrangement that was used. See Figure 3, page 16. The use of strain gage rosettes instead of the arrangement that was used would have allowed the computation of principal tensile stresses and also of the shear stresses. The tensile stress is found to be:

$$\sigma = \frac{\sigma_L + \sigma_T}{2}$$

2. Warping Stresses

Warping stresses are caused by a temperature gradient which exists through a concrete slab and tend to cause the edges of the slab to curl about the centroidal axis. In this investigation, the model was at all times in an enclosed room within which the temperature varied very slowly and never more than fifteen degrees Fahrenheit. The shallow depth of the slab would also permit rapid temperature adjustment throughout the slab. It was thus assumed that no temperature gradient existed and therefore that no warping stresses existed since none of the extreme temperature differentials that would normally be encountered on a highway were present. No advantage would be gained

by introducing such conditions into this investigation as only the effects of the load were of interest.

3. Expansion and Contraction Stresses

Expansion and contraction stresses are caused by changes in temperature and tend to cause expansion or contraction of the volume of the slab. However, if the slab is free to move on its subgrade, no stresses will develop as no friction is present to cause restraint to movement. Since also, the stresses caused by friction forces vary with length, it was assumed that such stresses within the model were insignificant. No other stresses were used or considered to be of any significance in this investigation due to the relatively short length of the model as compared with normal highway slabs. Therefore, only the strains caused by the simulated axle loading were used in the model analysis as they were the only significant strains present. Shrinkage strains were assumed to be present but in the area of the joints such strains should be expected to have no significant effect on the load strains because shrinkage strains at any one point in the interior of the slab should be uniform in effect.

III. MODEL TESTS

1. The Purpose

The model tests provided information to amplify and support the analytical analysis. A scale model of a representative section of a highway pavement was made. (See Plate 3, page 15. Strain gages of the A-7 SR-4 type were attached to the bottom of the slab in order to be able to read strain. See Plate 4, page 15, and Figure 3, page 16.

2. Model Development

Concrete used was designed to meet standards as called for by the Portland Cement Association (11, p. 16) for a three inch slump, with a maximum aggregate size of three quarters of an inch. A ratio of 5.5 gallons of water per sack of cement was used to conform to Portland Cement Association recommendations (11, p. 5). Type I or normal Portland Cement was used, which is suitable for pavement construction where no special conditions exist. Crushed and screened aggregate was used which was obtained from Corvallis Sand and Gravel, a local supplier of building materials. The aggregate was washed before using and the slab cured for four months before any tests were made.

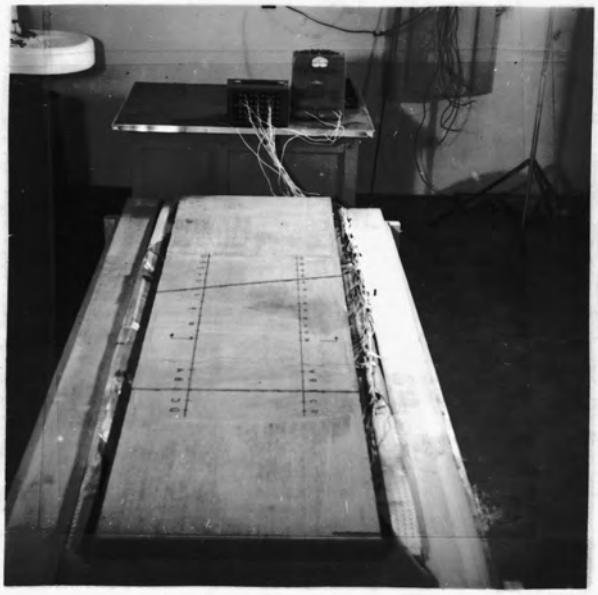

Plate 3. Model Slab

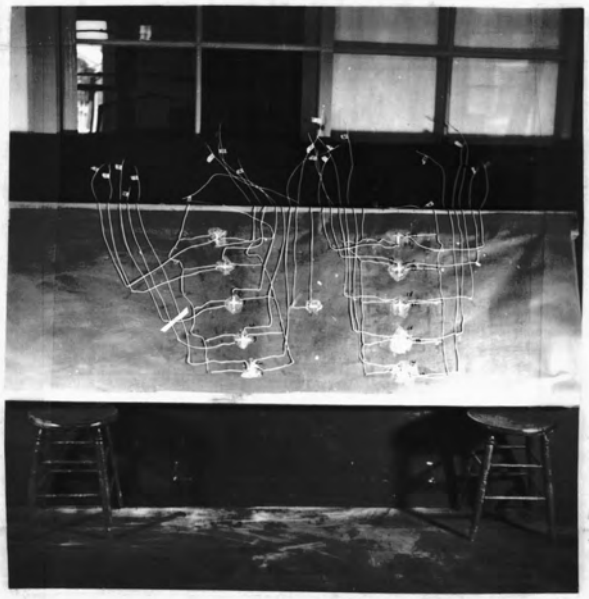

Plate 4. Strain Wiring Under the Model

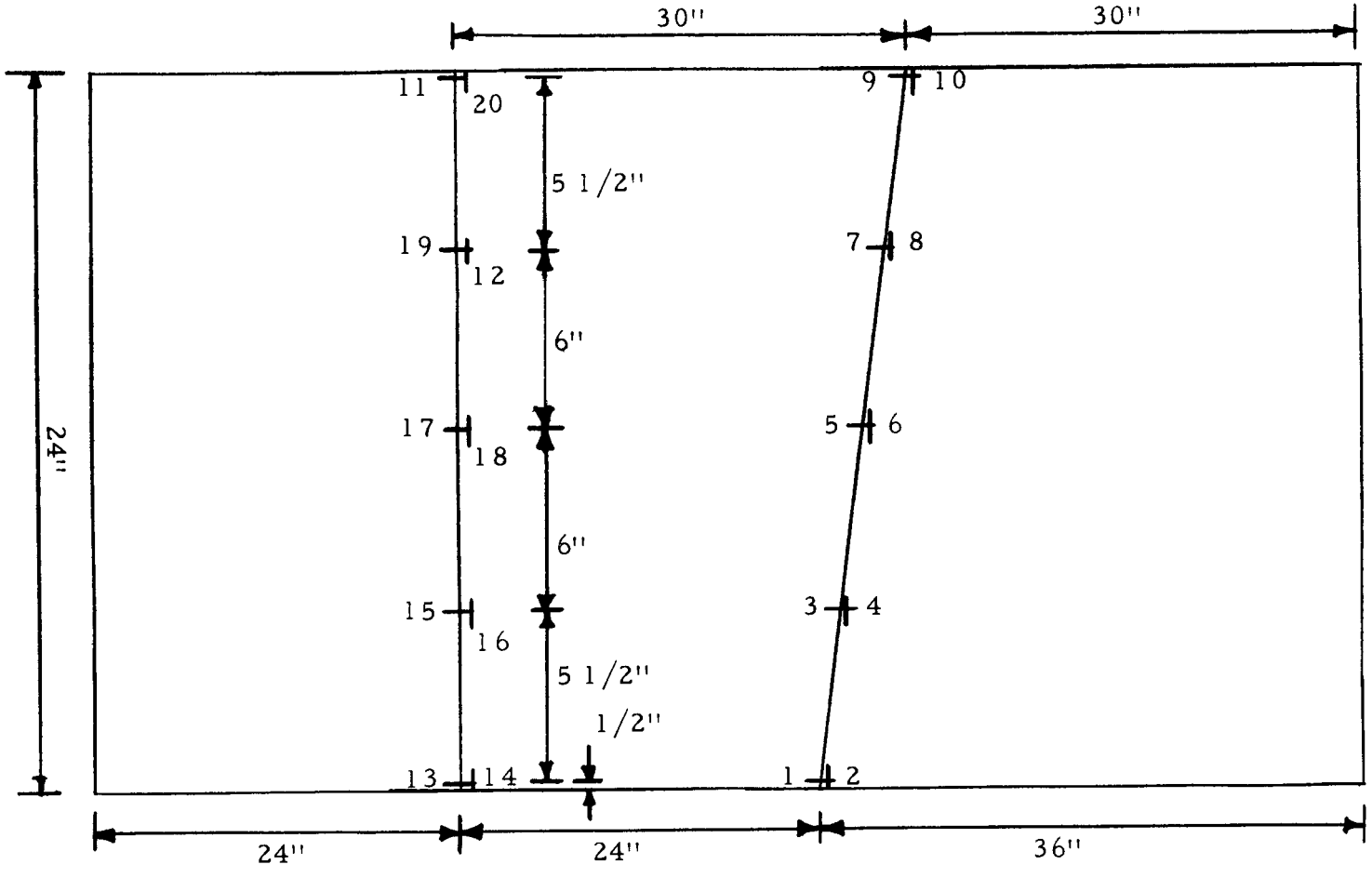

Figure 4. Location of Strain Gages.

The concrete slab had a volume of 2" x 24" x 84" which equals 2.33 feet^3.

For 3/4" maximum aggregate size, a 5 1/2 gallon sack mix will yield 3.91 feet^3 of concrete (11, p. 16), using the following percentages:

Aggregate: fine: 44% or 195 pounds per sack of cement

coarse: 56% or 250 pounds per sack of cement

Percentage to be used for required volume $\frac{2.33}{3.91} = 0.596$

fine: 195 x 0.596 = 116.0 pounds

coarse: 250 x 0.682 = 149.0 pounds

Water: 5.5 x 0.596 = 3.28 gallons

Cement: assume that one sack weighs 94 pounds (standard sack)

94 x 0.596 = 56.2 pounds

This configuration of the slab was selected as a representative section of a highway pavement twelve feet wide for one lane reduced by a factor of one sixth. The depth of the model was arbitrarily chosen as two inches.

2. Design of Axle and Loads

H 20 highway loading

2000 # / 75 #	8000 # / 300 #	actual / model

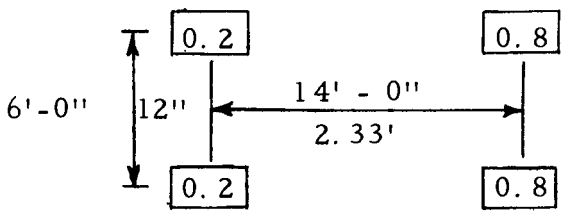

Figure 4. H 20 Highway Loading.

The use of a reduced load was required because of extremely weak subgrade. The wheel loading used was actually 198 pounds. This was done in order to produce strains large enough to generate discernable strain differences between successive positions of loads and at the same time use loads small enough to preclude any possibility of breaking the slab. Only one axle loading was used as it was found that for the configuration used the axle that was remote from the gage did not produce enough strain in the gage to be observed.

A well graded sand was initially used as a subgrade. Later a sheet of foam rubber two inches thick was used when it became apparent that the sand, which was confined in a box, did not permit enough deflection which resulted in extremely low strain gage readings. When the foam rubber laid over the sand was used as a subgrade, satisfactory strain readings were obtained.

The testing apparatus was designed in order to be able to read directly the strain in the concrete due to vertical loads applied to the top of the slab in the same manner that a wheel load of an axle of a vehicle would be applied. The axle spacing used was that of a standard H-20 truck with an axle width as shown (6, p. 84). A scale of one sixth of the actual dimension was selected for convenience.

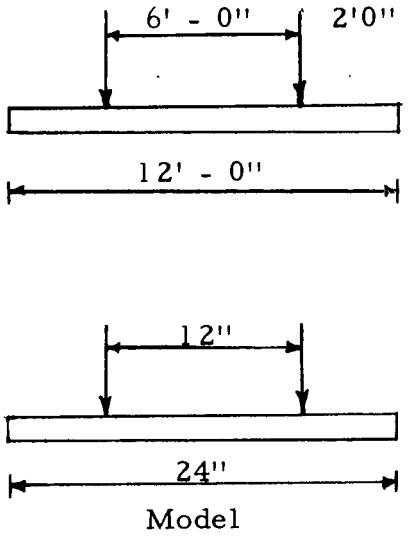

Figure 5. H-20 Highway Loading Diagram.

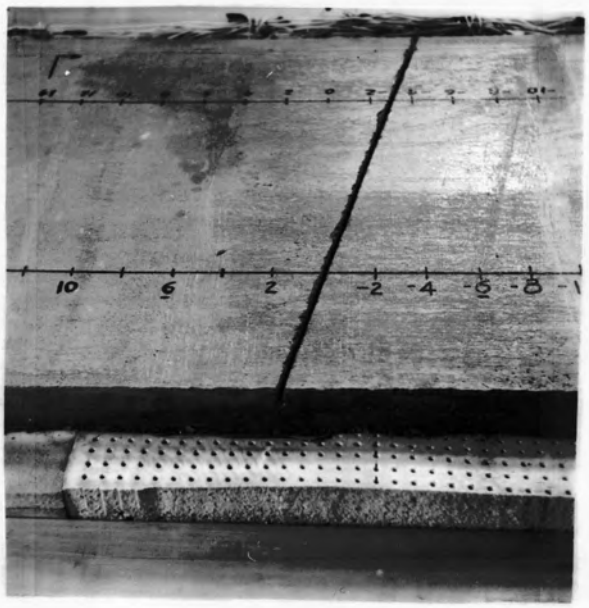

Plate 5. Skewed Joint

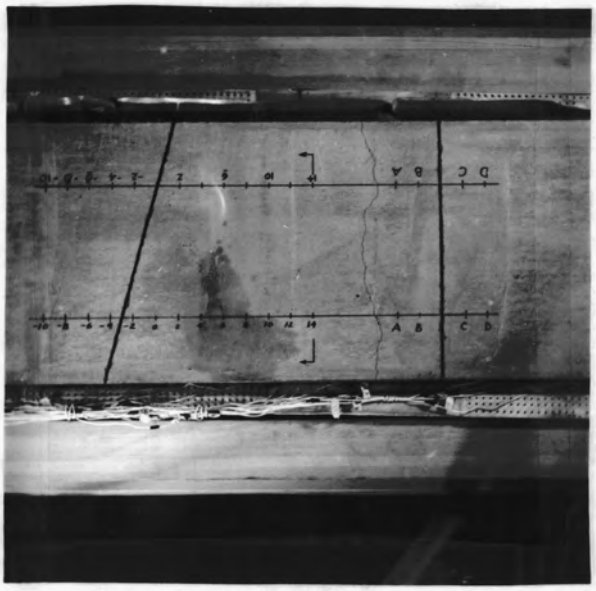

Plate 6. Joints and Load Positions

This scale was followed excepting for the depth of the slab where the one sixth size was thought to be too small to provide adequate strength and would also have caused construction difficulties.

The SR-4 strain gages were placed as shown in Figure 3, page 16. The configuration was used in order to be able to record longitudinal and transverse strain at each point. The normal or straight joint was also used in order to be able to make a comparison between the two types of joints. The brass fork (Figure 6, page 22), was used to assure positive contact between the concrete and the strain gages. The brass forks were individually tested to insure that they would transmit the strain without yielding.

Waterproof paper and wax was used to protect the strain gage from moisture contact and from the sand of the subgrade during the pouring and the curing of the concrete. The tines of the brass forks were punched through the paper and the concrete was poured directly onto the paper. When the concrete cured, the forks were firmly imbedded in the concrete. Periodic tests during curing showed that all the strain gages were functioning properly and normally. No adverse results to the wiring system or the gages were encountered during the construction of the slab. A comparison of strain readings taken after curing shows considerable internal strain on the gages which is believed to be caused by contraction of the slab during curing.

Brass Fork

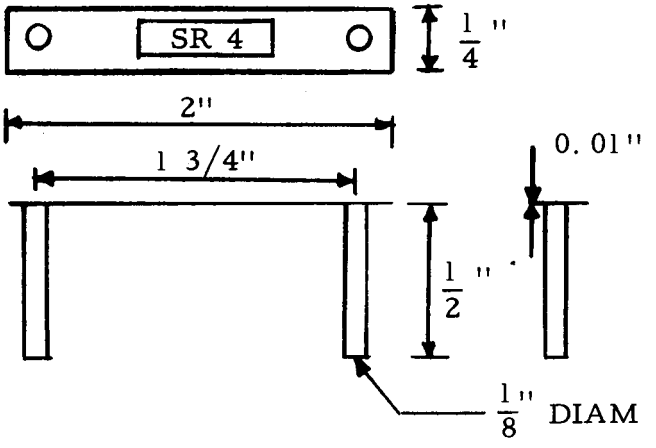

No Scale

Figure 6. Brass Fork.

The wiring system was designed so that all gages could be read from a single meter without disturbing the wiring. A standard Baldwin Meter was used which could be read to ten microinches. This method made possible rapid reading of the gages. See Plate 7, page 24.

3. Testing

After the slab had cured, each gage was tested with loads up to two hundred and ninety seven pounds applied in increments of thirty-three pounds. The use of thirty-three pounds as load increment was due solely to the available supply of weights which were copper bars of five and one half pounds each. This was done to determine if the strain plotted graphically against the load increments would prove linear. If this should occur, it would then show that the strain is proportional to the load. The results (Appendix B) indicate that all gages responded satisfactorily. Before each reading it was necessary to zero each gage to be read, since the no load or zero reading varied with each test. This was carefully done in every instance to insure the greatest possible accuracy. The zero of the gages was re-checked as the load was removed with no variance with the initial zero reading greater than five microinches was observed. Values of strain were adjusted to the average no load reading when the difference was greater than two microinches.

Plate 7. Strain Indicator and Switching Unit

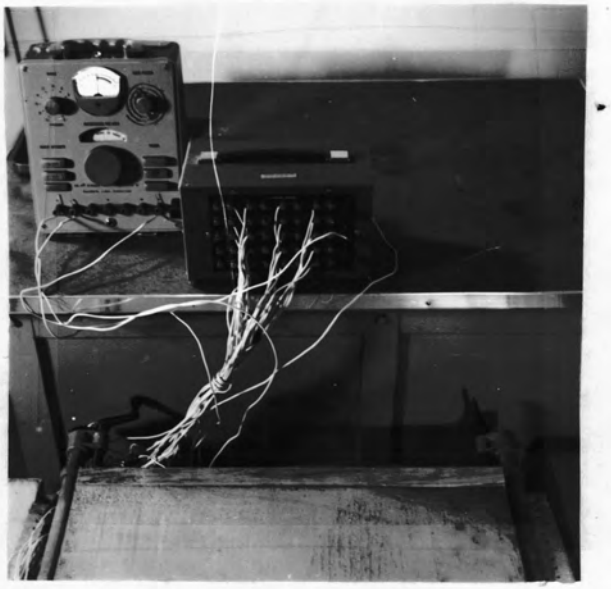

Plate 8. End Clamps and Wiring Connections

The model was tested by loading the slab with weights acting at successive stations as indicated in Figure 7, page 26. Each gage was read from A to D for the normal or straight joint. A loading of 198 pounds per wheel was used and no variation of the load was made. The results of the loadings were plotted before and after the joints were cut and the results are tabulated in Tables 1 and 2, pages 27 and 28.

After all tests were run on the solid slab, the joints were sawed one half inch deep with a skill saw. The joints were carefully plotted so that the saw cuts would be placed in the desired relation to the strain gages as indicated in Figure 7, page 26. The load tests were then run again in the same manner as all previous tests. See Tables 3 and 4, page 29.

An attempt was made to crack the slab clear through at the sawed joints. This was done in order to duplicate as closely as possible the conditions that would normally be expected to exist in a highway slab. Hydraulic jacks were placed on the joints; spreader bars of two by six planks were placed on one half inch by one eighth inch metal strips so that both planks and strips were long enough to completely cover the width of the slab. One end of the slab was then raised by placing a three quarter inch by three quarter inch by one eighth inch angle iron under the slab so that one end of the slab was slightly elevated. See Figures 8 and 9, page 30.

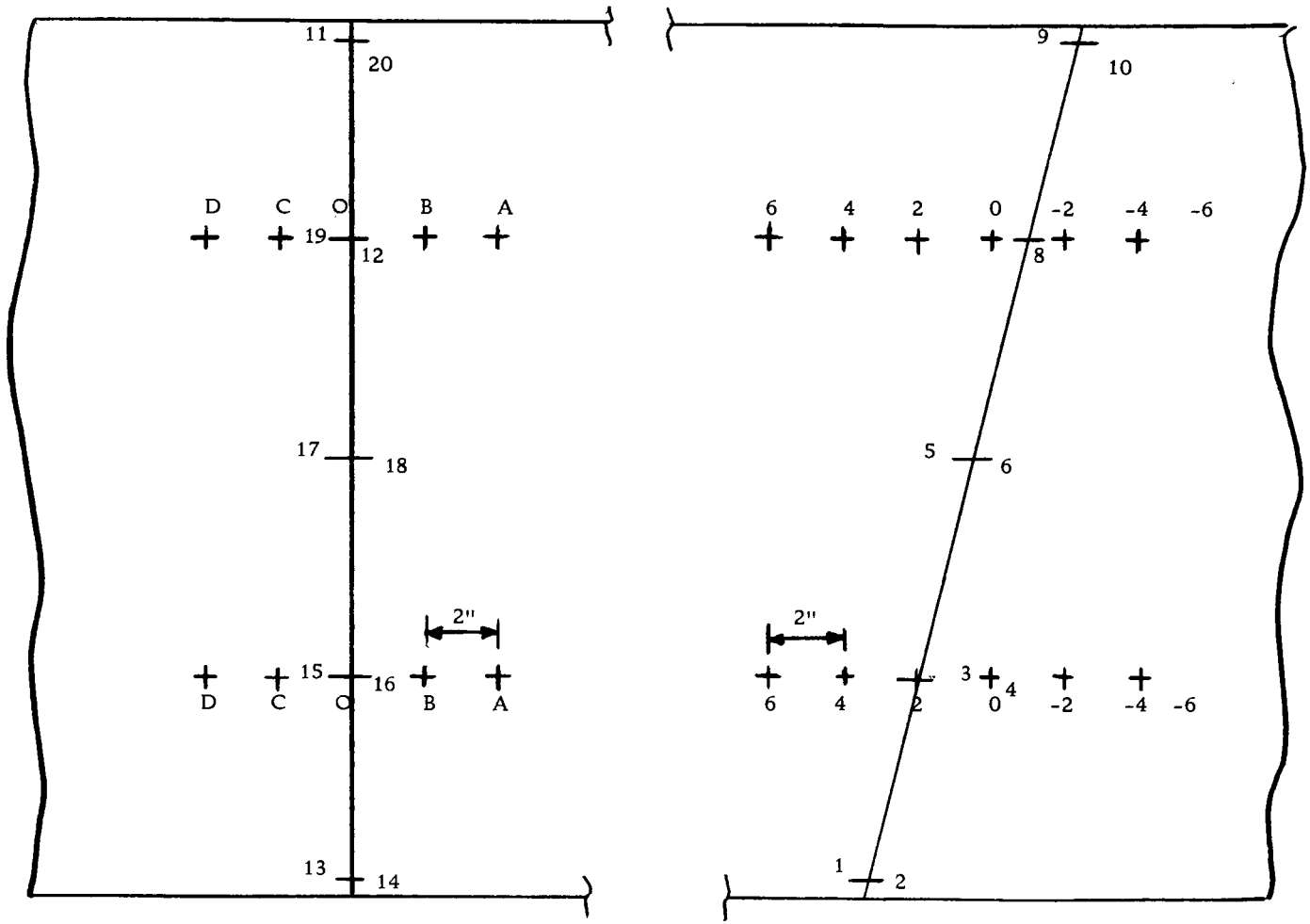

No Scale

Figure 7. Location of Loading Points.

Table 1. Skewed Joint Solid Slab.

Gage Number	Position							
	zero	-6	-4	-2	0	+2	+4	+6
1	17620	631	636	636	638	638	633	631
2	18730	728	728	723	724	720	719	719
3	17292	302	308	309	311	309	302	309
4	18721	713	714	718	718	714	710	709
5	16518	532	535	535	532	531	528	525
6	18614	609	604	604	604	604	600	601
7	17241	255	259	259	252	251	248	248
8	13490	489	489	491	488	487	479	480
9	19549	563	567	561	559	554	552	550
10	18536	521	519	521	520	521	518	519

Table 2. Normal Joint Solid Slab

Gage Number	Position					
	zero	A	B	O	C	D
11	14888	899	901	902	901	898
12	13776	770	771	774	773	778
13	18879	889	890	891	890	888
14	16616	612	612	615	618	619
15	15541	549	551	552	552	549
16	19061	060	060	062	064	066
17	15401	411	415	417	415	412
18	16035	029	029	030	032	037
19	17273	281	285	288	284	281
20	14522	521	522	523	523	529

Table 3. Skewed Joint Cut Slab.

Gage Number	Position							
	zero	+6	+4	+2	0	-2	-4	-6
1	17547	561	567	569	569	567	565	560
2	18679	667	668	668	670	670	672	672
3	17222	242	249	251	253	251	248	241
4	18658	649	652	655	659	658	655	654
5	16470	487	490	491	494	498	494	491
6	18551	541	541	544	546	547	548	549
7	17181	192	198	199	201	206	203	200
8	13349	340	339	342	344	350	351	350
9	19463	479	483	484	489	491	493	489
10	18485	471	469	470	470	471	471	471

Table 4. Normal Joint Cut Slab.

Gage Number	Position					
	zero	A	B	O	C	D
11	14864	887	888	887	883	878
12	13753	751	751	752	750	755
13	18872	899	900	901	900	890
14	16593	593	596	599	599	590
15	15490	508	510	513	509	503
16	19020	019	021	023	021	024
17	15382	401	403	402	398	394
18	16009	011	011	009	008	009
19	17227	241	247	249	245	240
20	14511	515	516	512	513	511

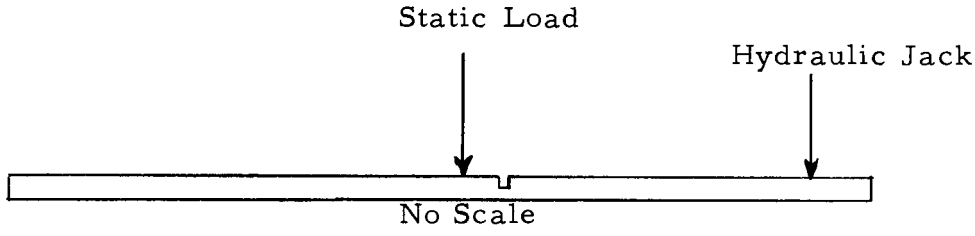

Figure 8. Loading Normal Joint.

This method of loading was used in order to produce tension on the underside of the slab. The center line longitudinal gages were read as load was applied by the jack. The jack worked against a steel framework and the load was applied vertically on the slab. The slab cracked approximately eight inches from the sawed joint and the cracks paralleled the joints in both cases. The normal joint was loaded by placing a static load on one side of the joint and jacking down on the end of the slab in the manner previously described.

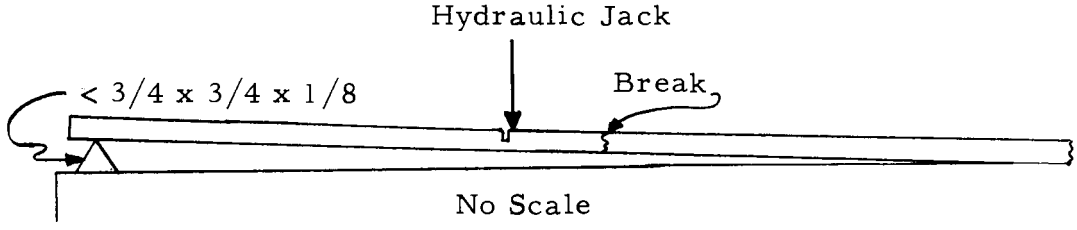

Figure 9. Loading Skewed Joint.

Again the slab cracked approximately eight inches from the joint and parallel to it. The gages recorded approximately 90 micro-inches of strain or 315 psi of stress. See Plate 9, page 32.

The ends of the slab were clamped with one inch pipes running the length of the slab. This was done to prevent separation of the joints when the slab was cracked in order to retain aggregate interlock. The method was successful in that no separation did occur.

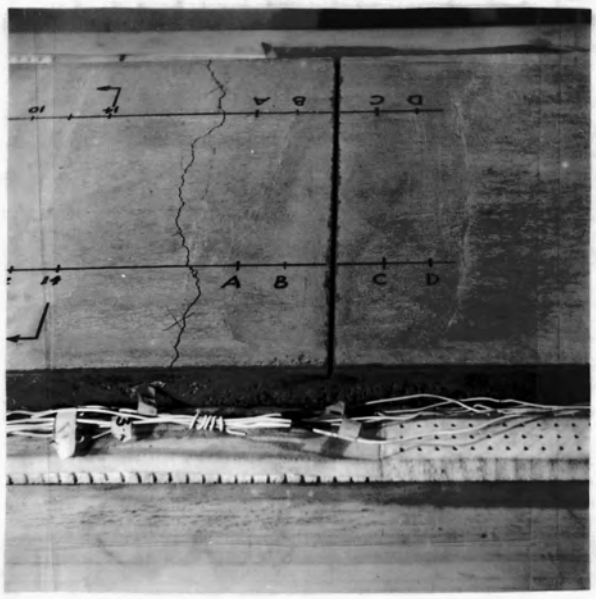

Plate 9. Normal Joint and Transverse Crack

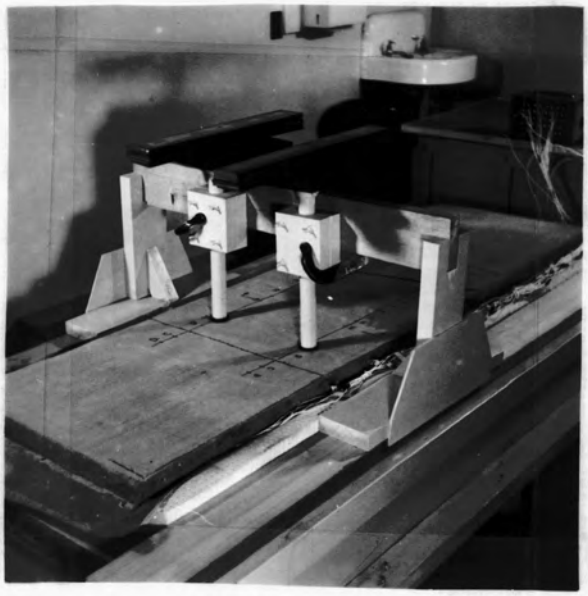

Plate 10. Loading Device With Weights

IV. CONCLUSIONS

The results of this investigation show that there is a correlation between the influence charts and the actual strain readings obtained by model studies. A comparison of the computed stress values and the predicted stress values show similar results when plotted graphically. See Table 5, page 34 and Table 6, page 35. While exactly similar values were seldom achieved, it does appear that the relative differences for any one position are reasonably constant for similar readings. See Table 7, page 37 and Table 8, page 28. Ideal or general conditions did not exist for the model tests that are assumed for the influence charts and other analytical studies.

Influence charts cannot account for any irregularities that may and usually do exist in a concrete slab. These irregularities are difficult to control and identify. The irregularities in this model can be such things as a weak aggregate specimen, void spaces, and poor interlock between batches of concrete. While these conditions can be controlled to some extent by careful planning and proper procedures, they can never be absolutely excluded.

In this investigation no attempt has been made to discover the reason for the discrepencies found between the predicted and computed stress values due to irregularities in the model. It is however, felt that the reason the slab failed to crack across the joints as

Table 5. Stress Tables, Solid Slab.

Strain Gage Stress
Influence Chart Stress

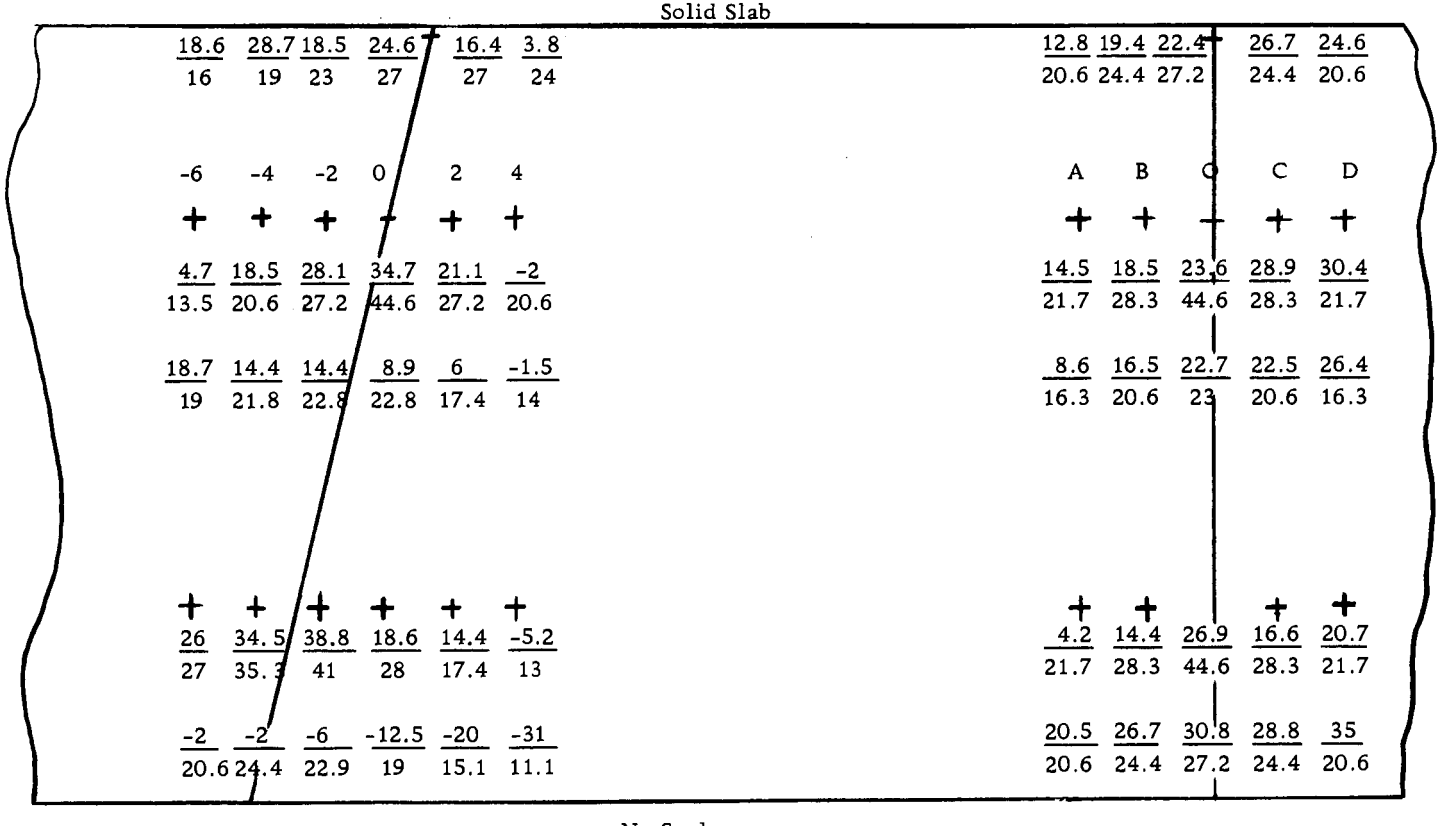

No Scale

Table 6. Stress Tables, Cut Slab.

Strain Gage Stress
Influence Chart Stress

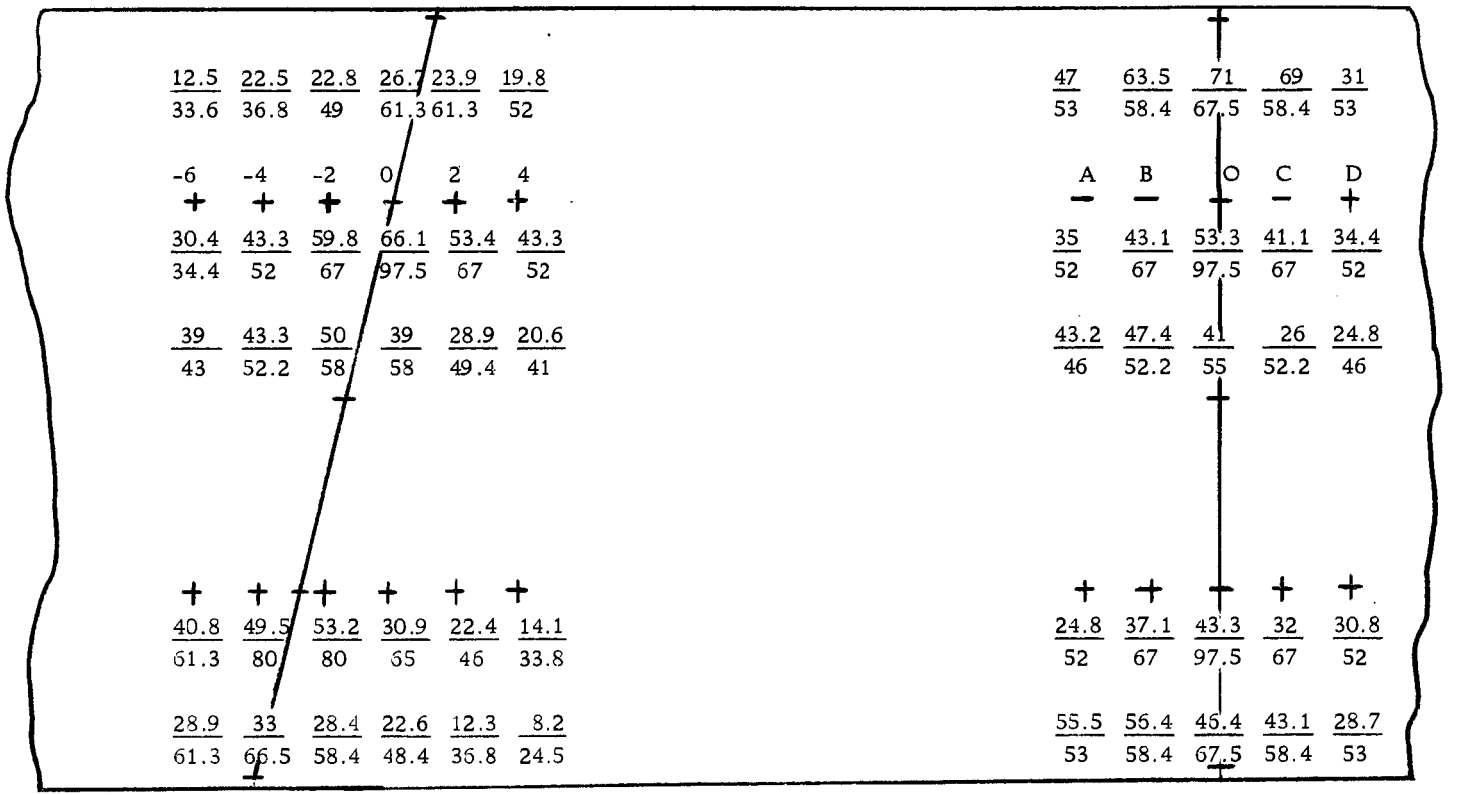

No Scale

7. Difference Influence Chart Stress and Strain Gage Stress

Table 7. Difference Between Influence Chart Stress and Strain Gage Stress ------ Solid Slab.

	Position				
Normal joint	A	B	O	C	D
13/14	- 7.8	- 5.0	- 4.8	+ 2.3	+ 4.0
15/16	- 7.2	- 9.8	-21.0	+ 0.6	+ 8.7
17/18	- 7.7	- 4.1	- 0.3	+ 1.9	+10.1
19/12	-17.5	-13.9	-17.7	-11.7	- 1.0
11/20	- 0.1	+ 2.3	+ 3.6	+ 4.4	+14.4
Skewed joint	-6	-4	-2	0	2	4
1/2	+ 2.6	+ 9.7	- 4.5	- 2.4	-10.6	-21.2
3/4	- 8.8	- 2.1	+ 0.8	- 9.9	- 6.1	-22.0
5/6	- 0.3	- 7.4	- 8.4	-13.9	-11.4	-15.5
7/8	- 1.0	- 0.8	- 2.2	- 9.4	- 3.0	-18.2
9/10	-22.6	-26.4	-28.9	-31.5	-35.1	-42.1

Influence Chart Stress used as zero point.

Table 8. Difference Between Influence Chart Stress and Strain Gage Stress ------- Cut Slab

	Position				
Normal joint	A	B	O	C	D
13/14	- 6	+ 5.1	+ 3.5	+10.6	-22
15/16	-17	-23.9	-44.2	-25.9	-17.6
17/18	- 2.8	- 4.8	-14	-26.2	-21.2
19/12	-27.2	-29.9	-54.2	-35	-21.2
11/20	+ 2.5	- 2.0	-21.1	-15.1	-24.3

Skewed joint	-6	-4	-2	0	2	4
1/2	-21.1	-14.3	-26.2	-34.6	-37.4	-32.2
3/4	- 4.0	- 8.7	- 7.2	-31.4	-13.6	- 8.7
5/6	- 4.0	- 8.7	- 8	-19	-20.5	-20.4
7/8	-20.5	-30.5	-26.8	-34.1	-23.9	-19.7
9/10	-32.9	-33.5	-30	-23.8	-24.5	-16.3

Influence Chart Stress used as zero point.

planned was due to the brass strips which held the strain gages acting as reinforcing. See Figure 6, page 22. These strips are felt to have carried a portion of the strain which affected the capabilities of the reduced cross section in such a manner as to allow the reduced cross section to carry a greater strain than the regular cross section.

Another irregularity may have been caused by poor binding between the brass forks which held the strain gages and the concrete; though no creeping of the gages was observed. Any irregularity could cause a reading to be excessively high or excessively low. So long as constant relative reading exists between the analytical or predicted value and the model value, the behavior of the slab may be said to be conforming to the analytical prediction. Since in this investigation, only the change in the stress pattern between the skewed and the normal configuration is of interest, the irregularities need not be of concern so long as the gages react in the proper manner to load. That is, that the strain-load relationship remain linear.

The edge conditions present the greatest relative differences between the influence charts and the strain readings. See Table 5, page 34 and Table 6, page 36. For the interior positions the predicted and model readings are relatively closer in value. In all cases, however, nearly the same quantitative relation exists between computed and predicted results for any one set of gages at a particular

position for either the cut condition or for the solid condition. See Table 7, page 36 and Table 8, page 37.

The values of compressive transverse strains indicate that there is little or no transverse bending in the model. This is probably due to the narrowness and to the stiffness of the slab. Almost all bending appears to be in the longitudinal direction.

The assumed value of Poisson's Ratio may not be the actual value and could be a cause of the discrepancies between strain gage stress and influence chart stress. With compressive transverse strains and an erroneous value of μ, a low stress value could result for many positions. The transverse gages at the edges of the slab may be suspect in that they appear to register strains that, in some cases, do not seem reasonable when compared with other gage readings. No gage readings were ignored and the actual values were used as this is what the model tests produced. See Figure 39, page 85 and Figure 43, page 89.

The influence chart stresses for the cracked condition indicate that the same relative stress pattern exists as in the solid and sawed condition. See Table 5, page 34, Table 6, page 35, Table 9, page 40, and Table 7, page 36. The stresses are lower than in the sawed state; this is to be expected as no transfer of bending would occur across a cracked joint.

Table 7. Stress Tables, Cracked Slab.

Influence Chart Stresses Only

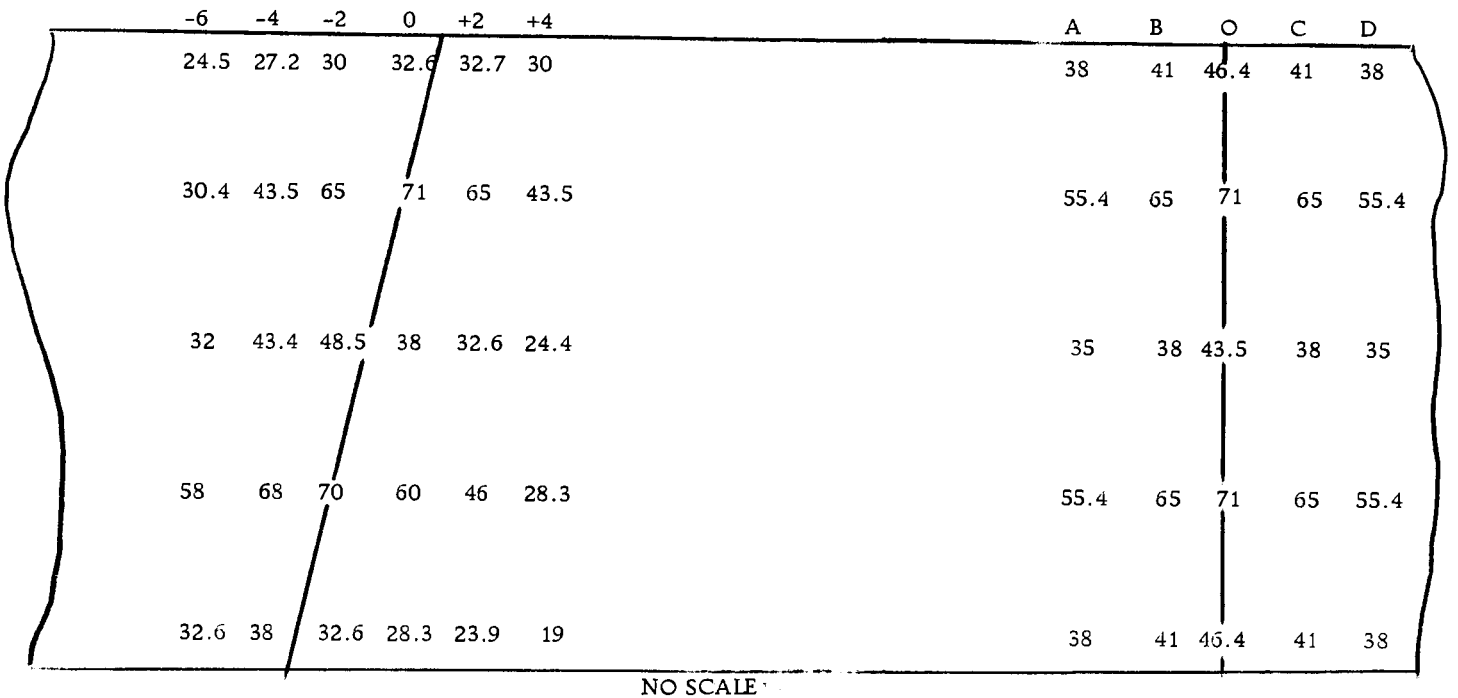

A study of Table 6, page 35 shows that the stress on the skewed joint will be considerably less than that occurring when the joint is perpendicular to the centerline of the slab. This is caused by the fact that the loads do not cross the joint at the same time so the entire axle weight is not transferred from one slab to the next at the same time.

While no test was made utilizing a moving load, it can be assumed from the tests made that the impact stresses caused by a moving load would show the same relative stress pattern to develop across a joint as that caused by a series of static loadings such as were used in this investigation.

For any point directly under a load, there does not appear to be any change in the stress developed for either type of joint. In the model tests the skewed joint appeared to reduce the impact stresses where the normal joint configuration would not do so for an axle load moving across the joint.

Further study utilizing strain gage rosettes would probably produce better correlation between strain gage stress and influence chart stress. The transfer of load across the cracked joint could not be observed on the model. Placing strain gage rosettes on both sides of the joint but not across the joint would permit an investigation of the transfer of load across a joint that was not possible in this

analysis, since only one set of strain gages were used and no differential strain readings across a joint were possible.

BIBLIOGRAPHY

1. American Association State Highway Officials road test. Washington, D. C., 1962. 352 p. (Highway Research Board of the NASNRC Division of Engineering and Industrial Research, publication no. 954)

2. Bradbury, Royall D. Reinforced concrete pavements. York, Pa., Maple Press, 1938. 190 p.

3. Cooley, R. H. The case for skewed joints. In: Concrete pavement design and performance studies, 1960. Washington, D. C., 1960. p. 113-118, (National Research Council. publication no. 812. Highway Research Board. Bulletin 274)

4. Grinter, L. E. Design of the reinforced concrete roadway slab. College station, 1931. 88 p. (Texas. Engineering Experiment Station. Bulletin 39)

5. Matson, Theodore M., Wilbur S. Smith and Frederick W. Hurd. Traffic engineering. New York, McGraw-Hill, 1955. 647 p.

6. Oregon. State Highway Department. Standard specifications for highway bridge construction. Salem, Oregon State Highway Commission, 1954. 181 p.

7. Pickett, Gerald, et al. Deflection, movements, and reactive pressures for concrete pavements. Manhattan, 1951. 123 p. (Kansas. State Experiment Station. Bulletin 65)

8. Pickett, Gerald and G. K. Ray. Influence charts for concrete pavements. Manhattan, Oct. 15, 1951. 24 p. (Kansas. State Experiment Station. Supplement to Bulletin 65)

9. _____. Influence charts for concrete pavements. Transactions, American Society of Civil Engineers 116:49-73. 1951.

10. Portland Cement Association, Chicago. Concrete pavement design for roads and streets carrying all classes of traffic. Chicago, 1951. 87 p.

11. _____. Design and control of concrete mixtures. 10th ed. Chicago, 1952. 68 p.

12. Ritter, Leo J., Jr. and Radnor J. Paquette. Highway engineering. 2d ed. New York, Ronald Press, 1960. 751 p.

13. Seely, Fred B. and James O. Smith. Advanced mechanics of materials. New York, Wiley, 1952. 680 p.

14. Spangler, M. J. Stresses in corner region of concrete pavements. Ames, 1942. 96 p. (Iowa. Engineering Experiment Station. Bulletin 157)

15. Timoshenko, Stephen P. and S. Woinowsky-Krieger. Theory of plates and shells. 2d ed. New York, McGraw-Hill, 1959. 580 p.

16. Westergaard, H. M. Stresses in concrete pavements computed by theoretical analysis. Public Roads 7(2):25-35. April, 1926.

17. _____. Theory of concrete pavement design. Proceedings of the Highway Research Board 1927. p. 177 - 181.

18. Yoder, E. J. Principles of pavement design. New York, Wiley, 1959. 569 p.

APPENDIX A

DEFINITIONS

E	Modulus of elasticity (pounds per square inch).
ϵ	Strain or elongation (inches per inch).
σ	Stress (pounds per square inch).
μ	Poisson's ratio.
h	Height (inches).
k	Modulus of subgrade reaction (pounds per cubic inch).
l	Relative stiffness (inches).
σ_T	Transverse stress.
σ_L	Longitudinal stress.
P	Unit load (pounds per square inch).
M	Moment (inch - pounds).
N	Number of squares.
Δ	Deflection (inches).

APPENDIX B

Test Data

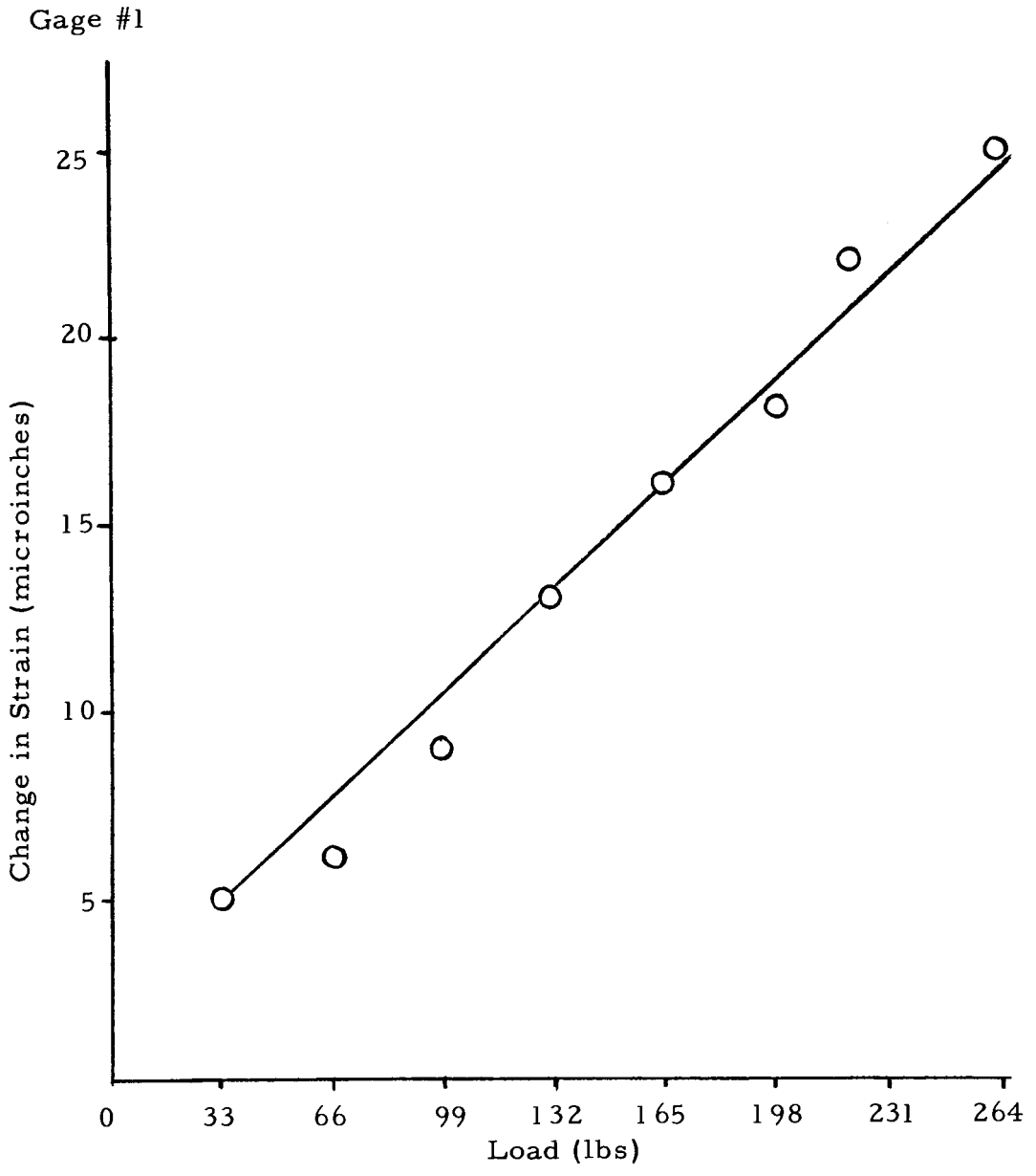

Load (lbs)	Gage reading
0	17663
33	17668
66	17669
99	17672
132	17676
165	17679
198	17681
231	17685
264	17688

Figure 10. Load versus Strain.

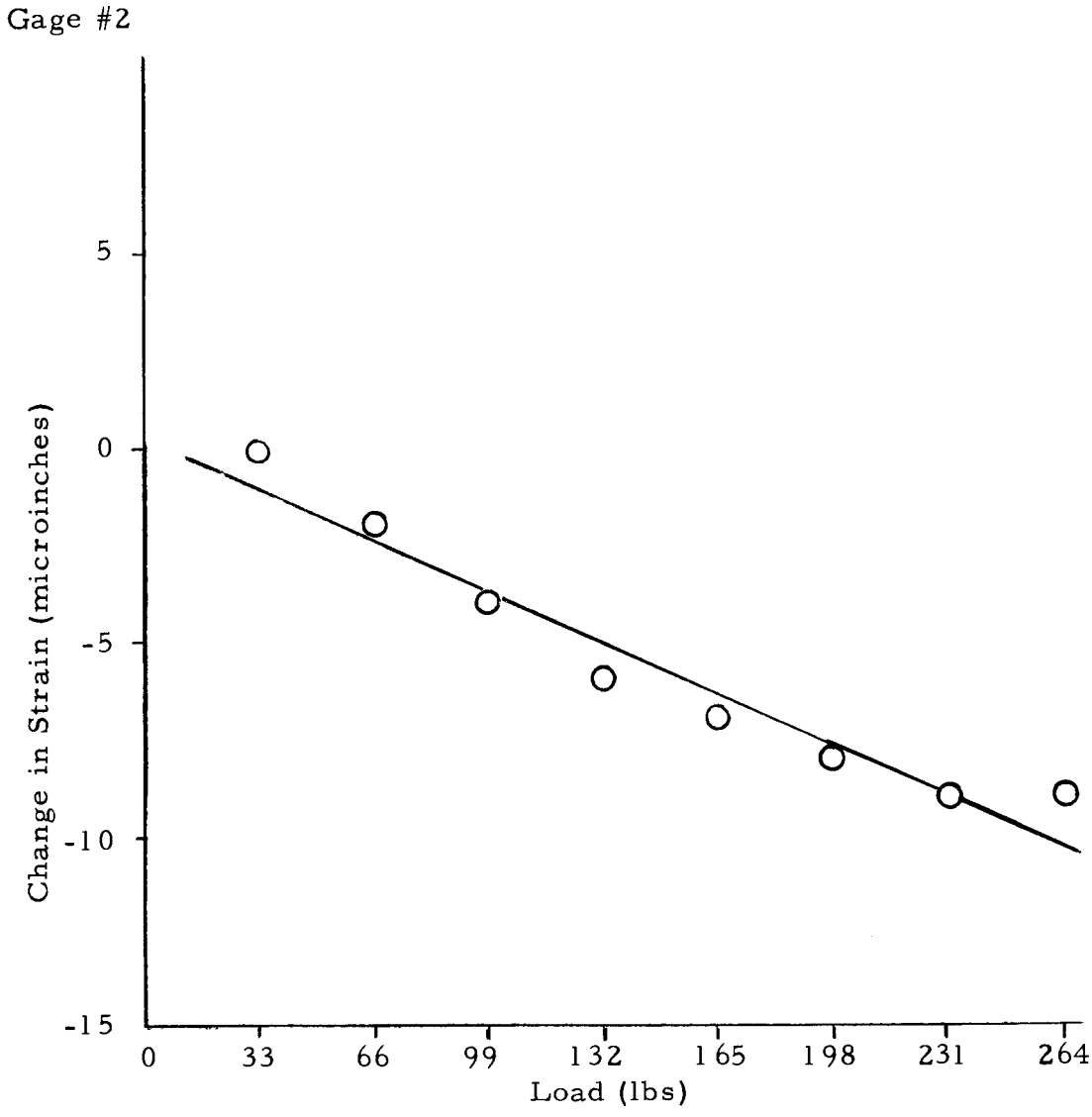

Load (lbs)	Gage Reading
0	18759
33	18759
66	18757
99	18755
132	18753
165	18752
198	18751
231	18750
264	18750

Figure 11. Load versus Strain.

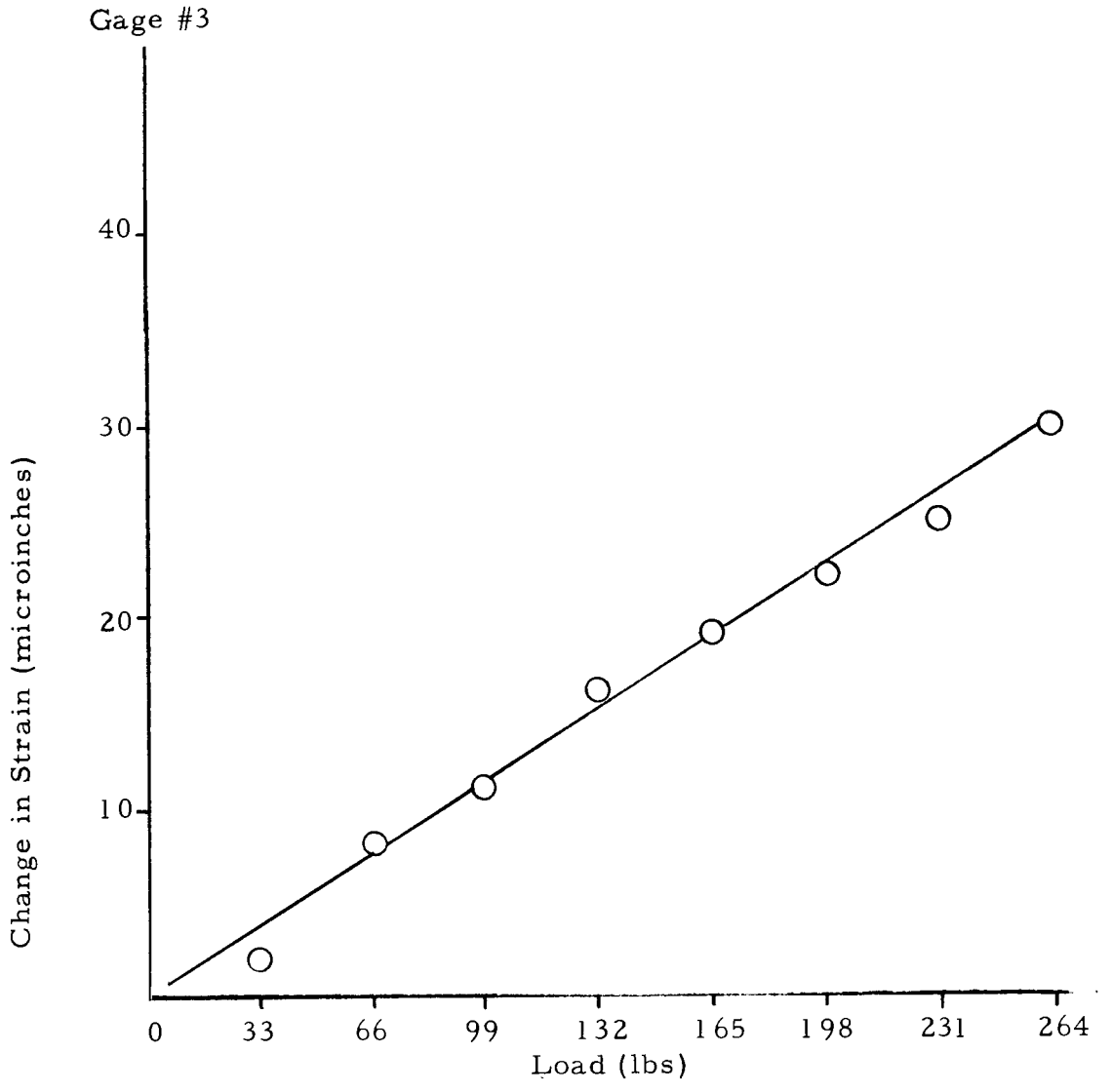

Load (lbs)	Gage Reading
0	17319
33	17321
66	17327
99	17330
132	17335
165	17338
198	17341
231	17344
264	17349

Figure 12. Load versus Strain.

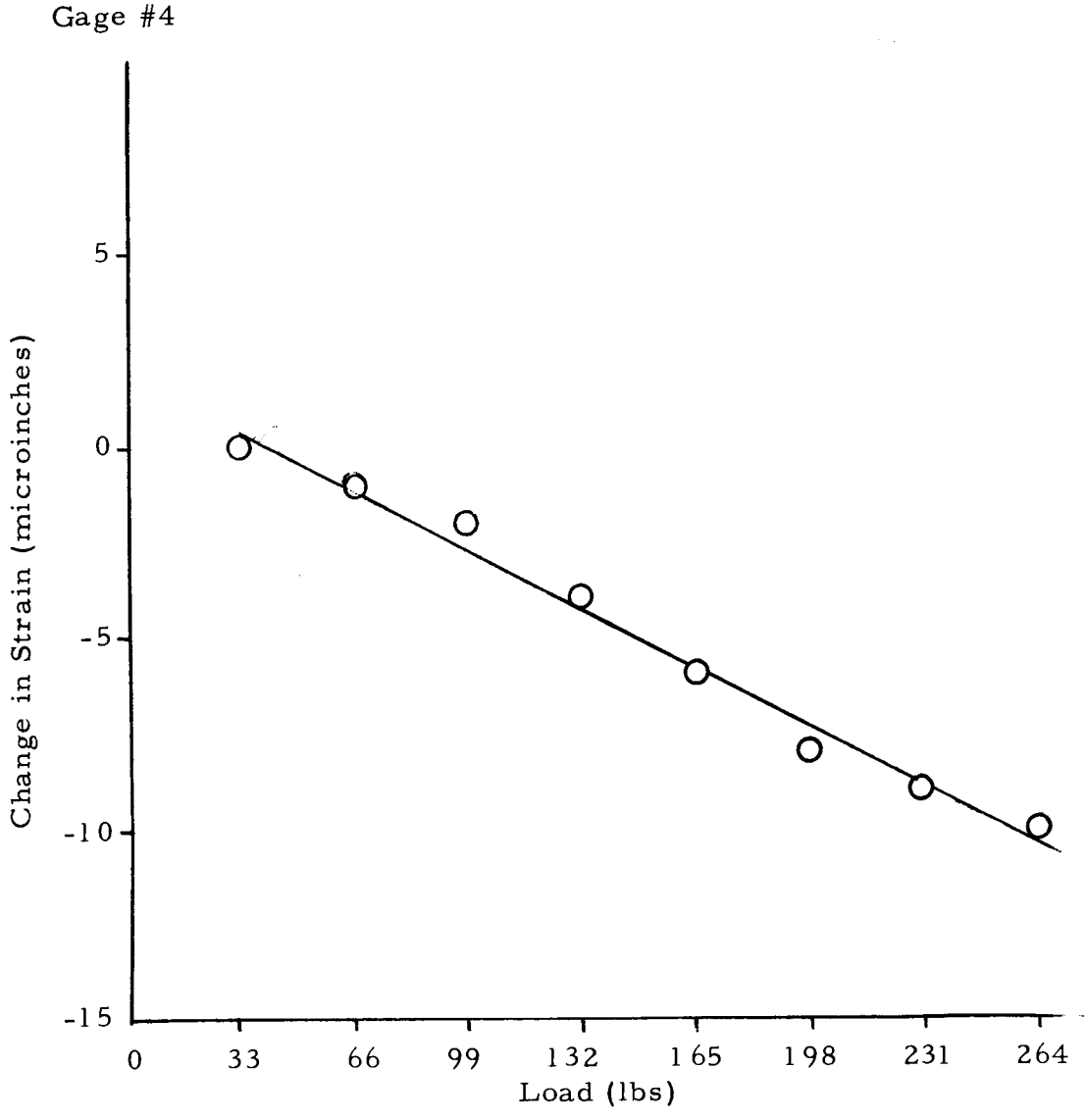

Laod (lbs)	Gage Reading
0	18751
33	18751
66	18750
99	18749
132	18747
165	18745
198	18743
231	19741
264	18740

Figure 13. Load versus Strain.

Gage #5

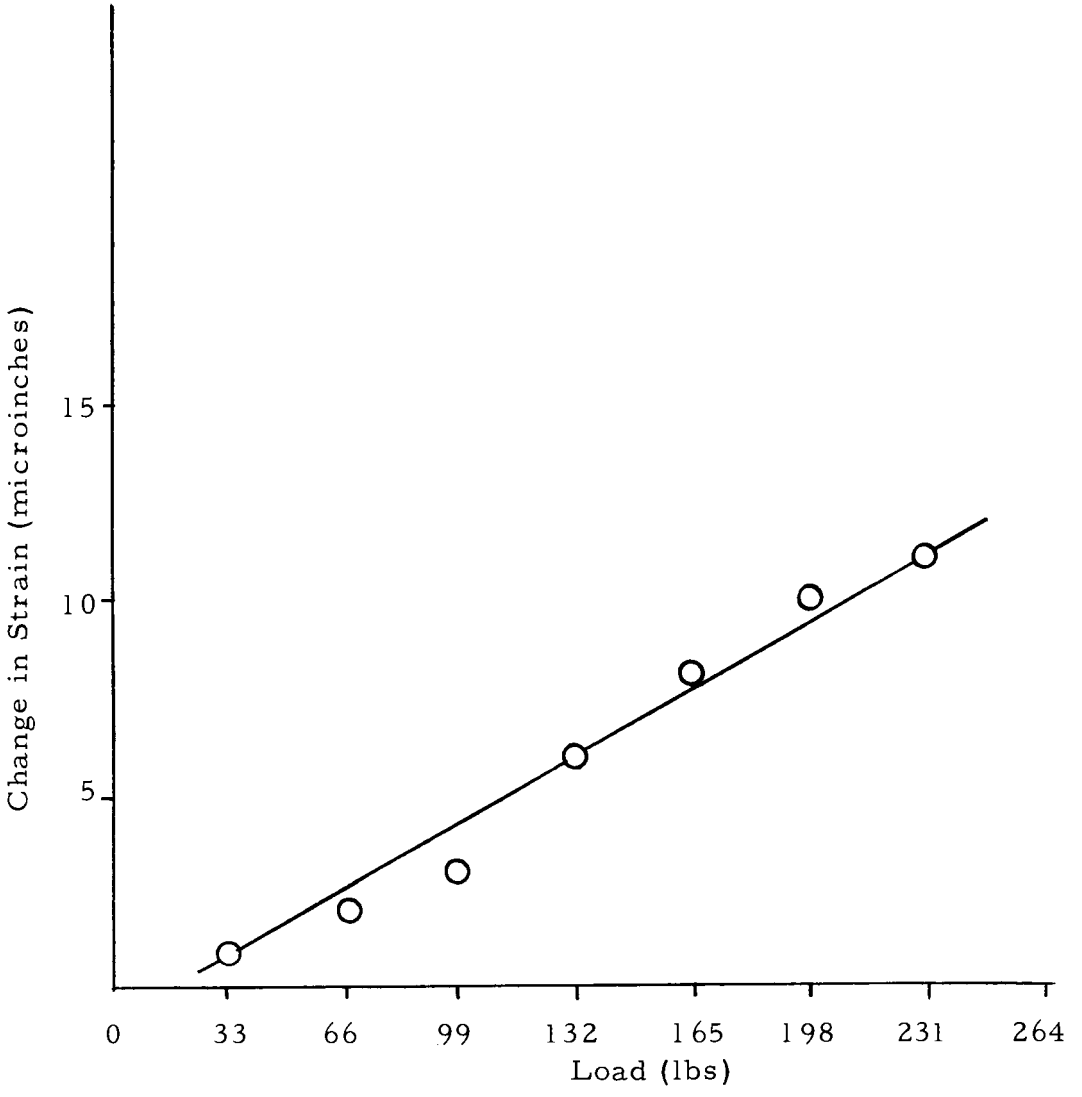

Load(lbs)	Gage reading
0	16560
33	16561
66	16562
99	16563
132	16566
165	16568
198	16570
231	16571

Figure 14. Load versus Strain.

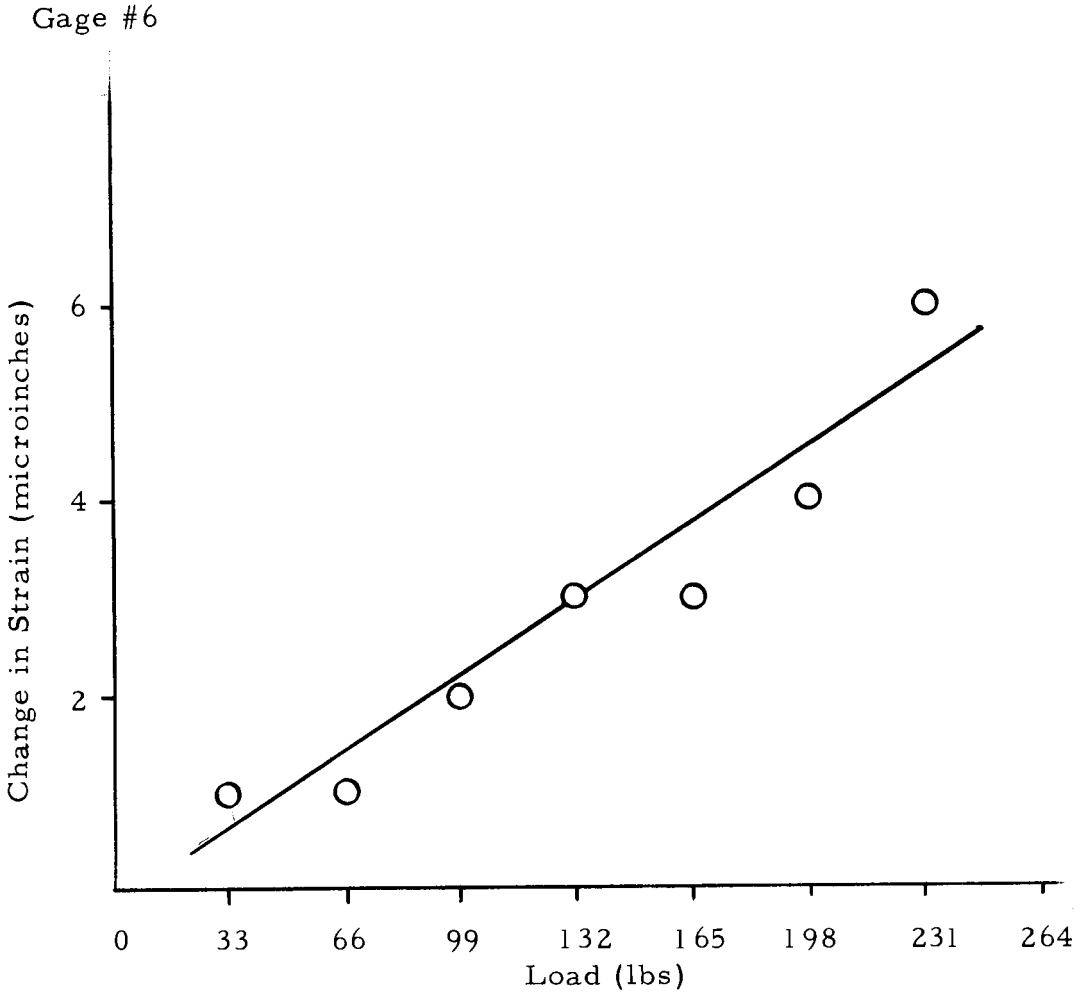

Load (lbs)	Gage Readings
0	18654
33	18655
66	18655
99	18656
132	18657
165	18657
198	18658
231	18660

Figure 15. Load versus Strain.

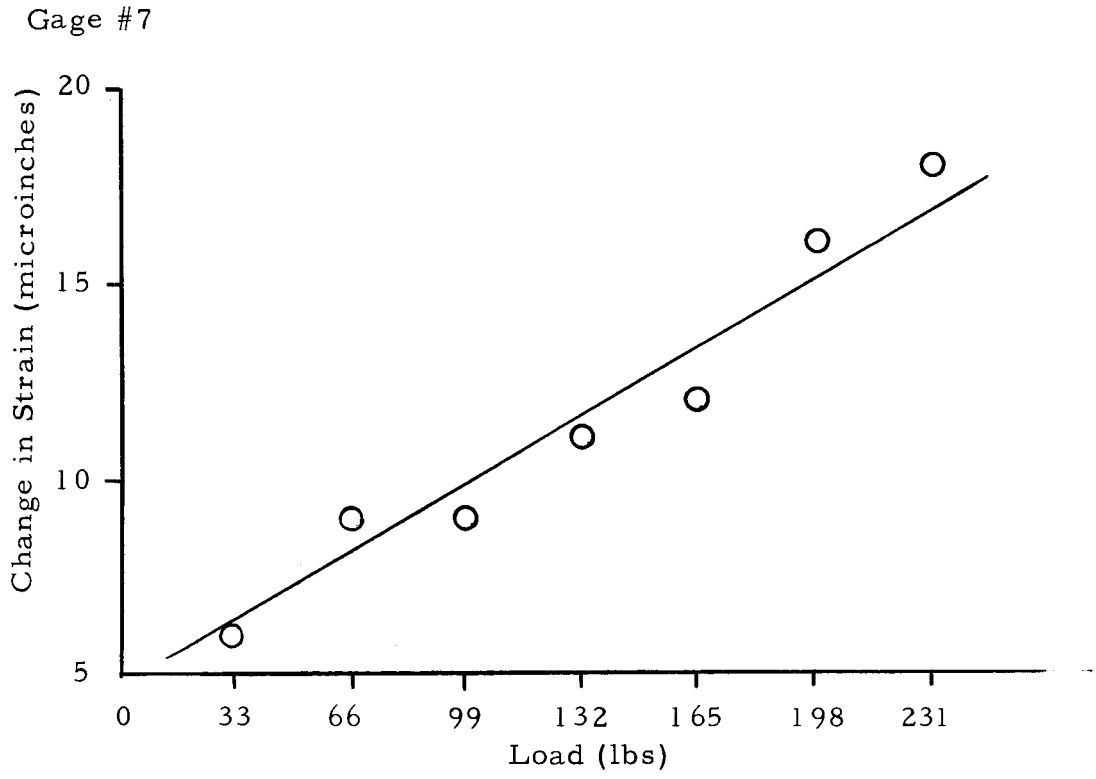

Load (lbs)	Gage Readings
0	17288
33	17289
66	17292
99	17292
132	17294
165	17295
198	17299
231	17301

Figure 16. Load versus Strain.

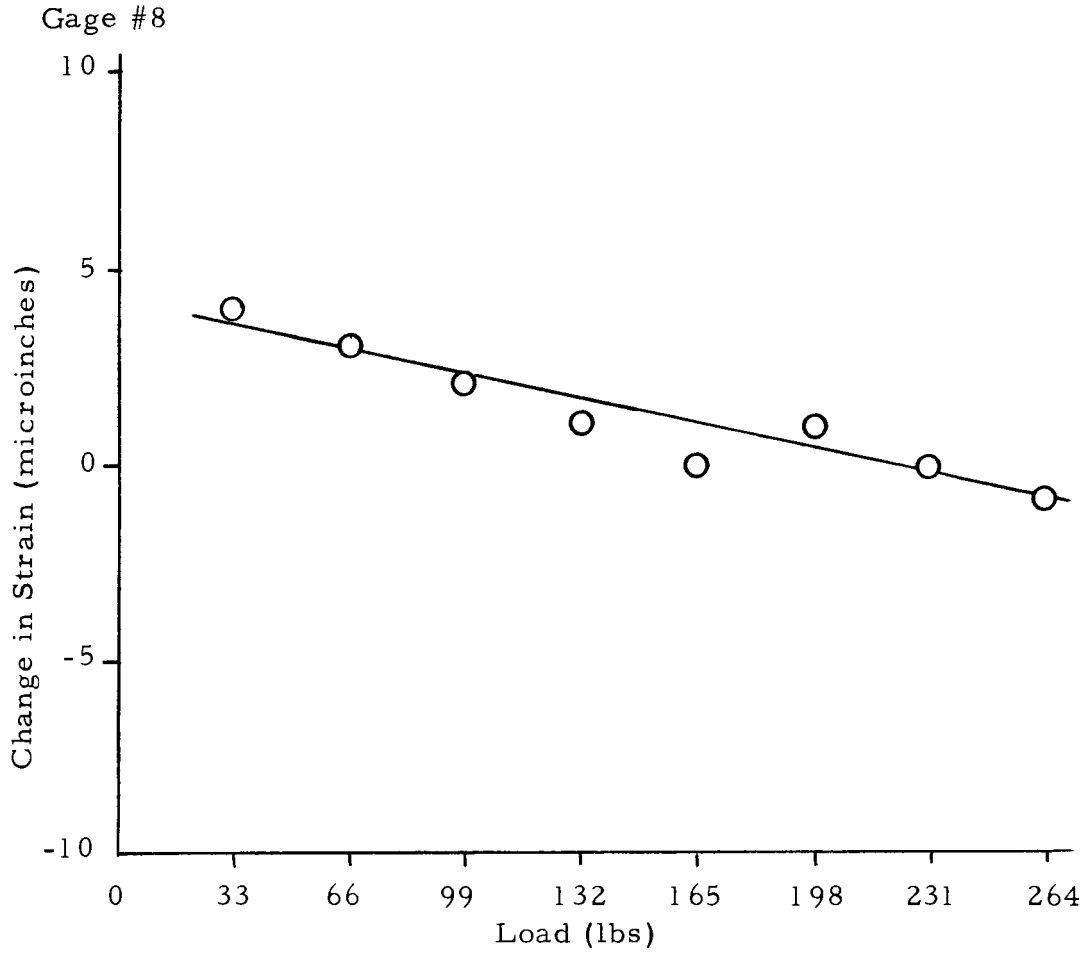

Load (lbs)	Gage Readings
0	13448
33	13452
66	13451
99	13450
132	13449
165	13448
198	13449
231	13448
264	13447

Figure 17. Load versus Strain.

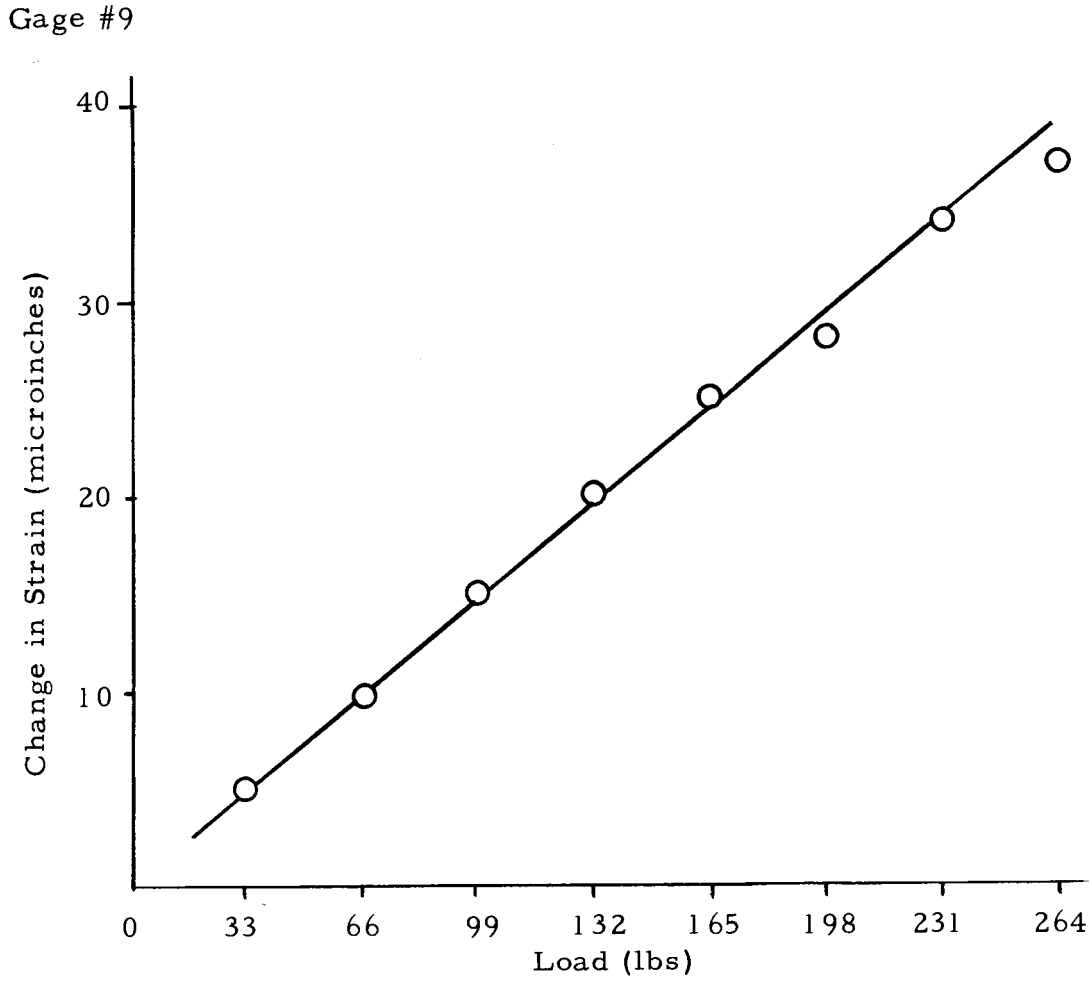

Load (lbs)	Gage Readings
0	19574
33	19579
66	19584
99	19589
132	19594
165	19599
198	19602
231	19608
264	19611

Figure 18. Load versus Strain.

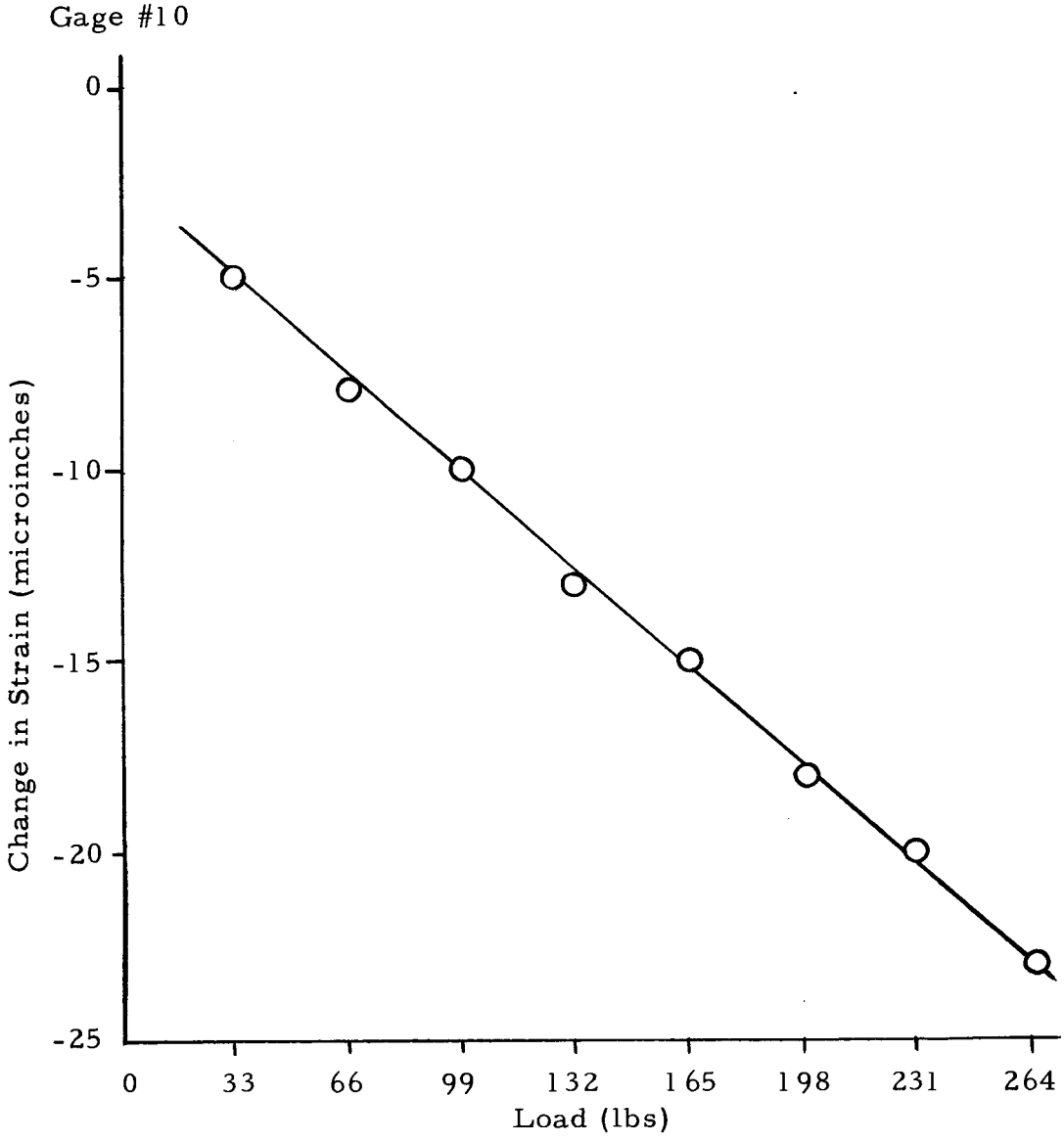

Load (lbs)	Gage Readings
0	18549
33	18544
66	18541
99	18539
132	18536
165	18534
198	18531
264	18526

Figure 19. Load versus Strain.

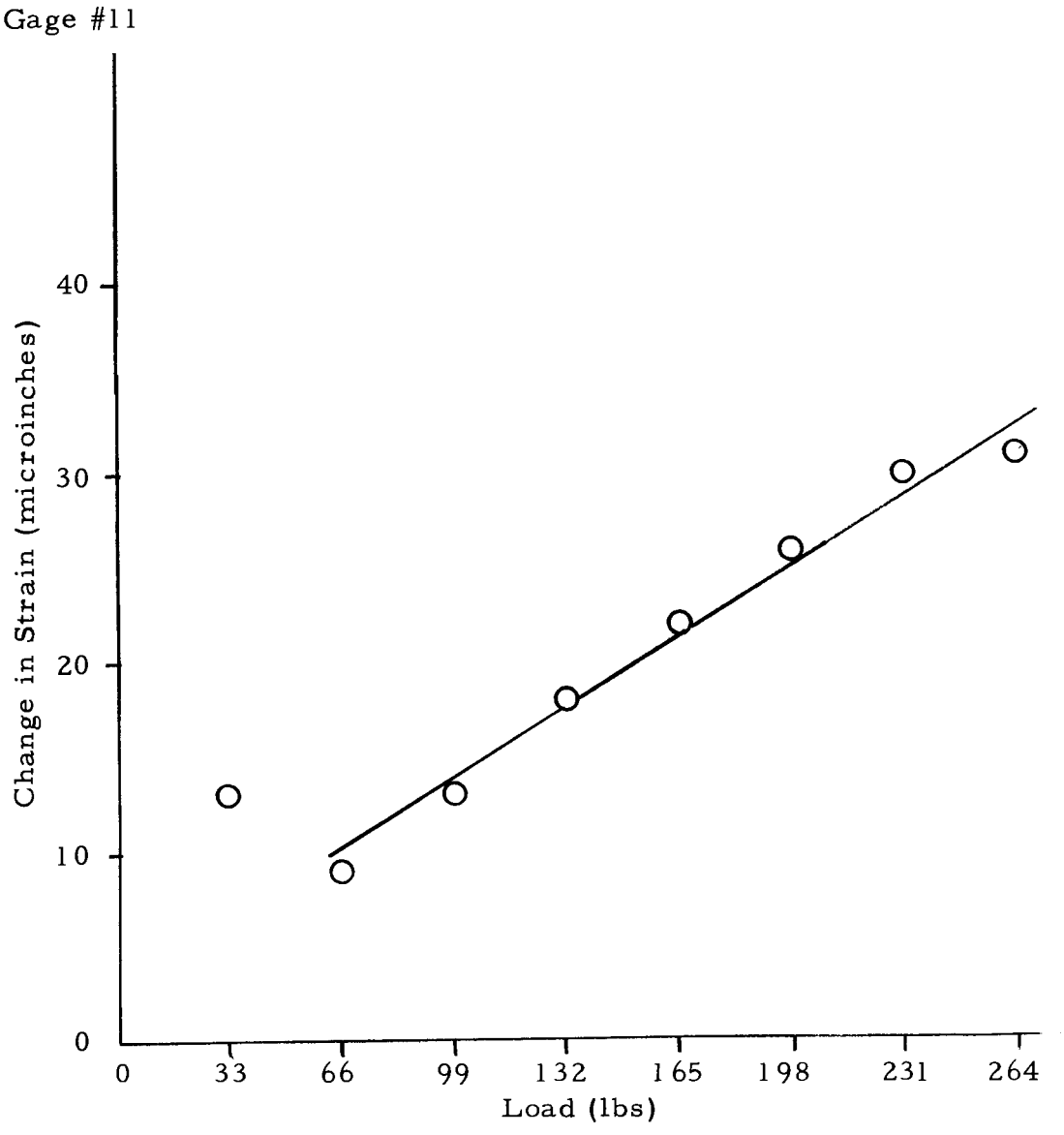

Load (lbs)	Gage Readings
0	14918
33	14931
66	14927
99	14931
132	14936
165	14940
198	14944
231	14948
264	14949

Figure 20. Load versus Strain.

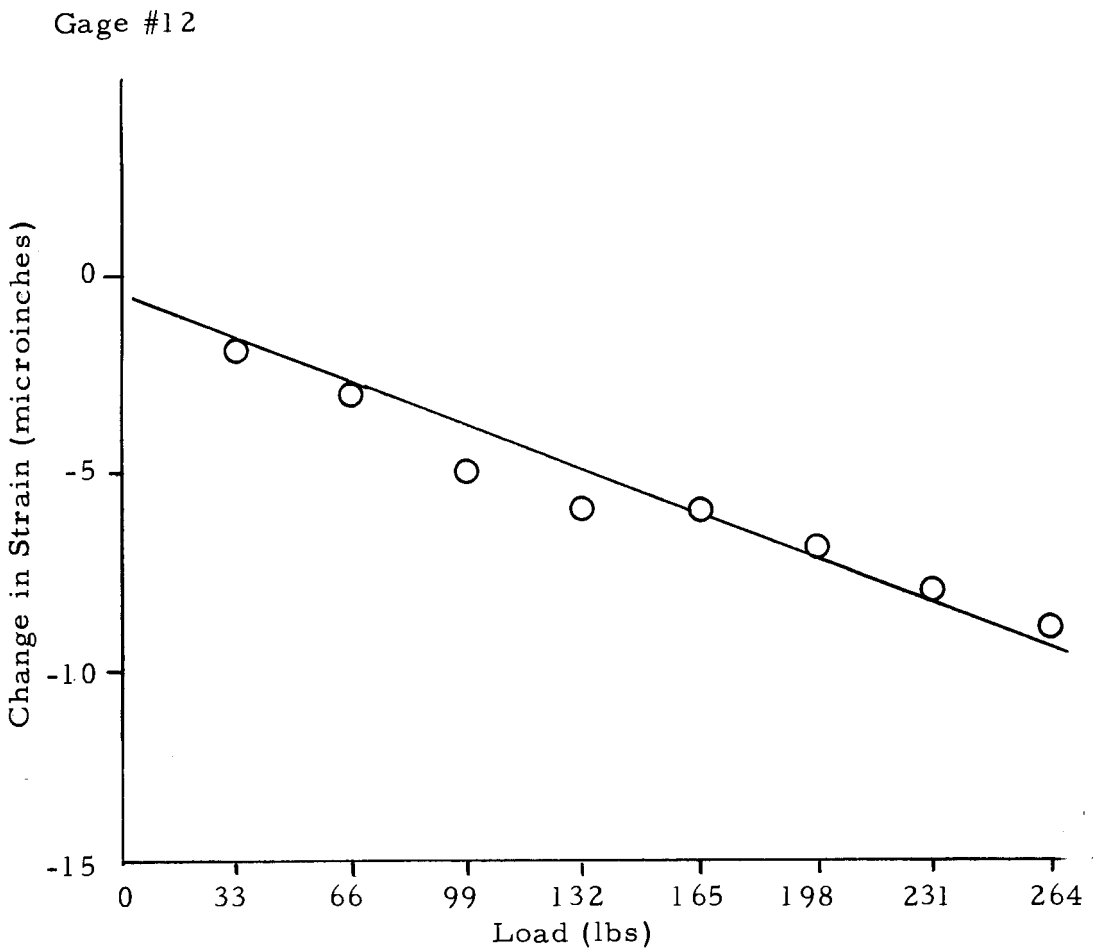

Load (lbs)	Gage Readings
0	13817
33	13815
66	13814
99	13812
132	13811
165	13811
198	13810
231	13809
264	13808

Figure 21. Load versus Strain.

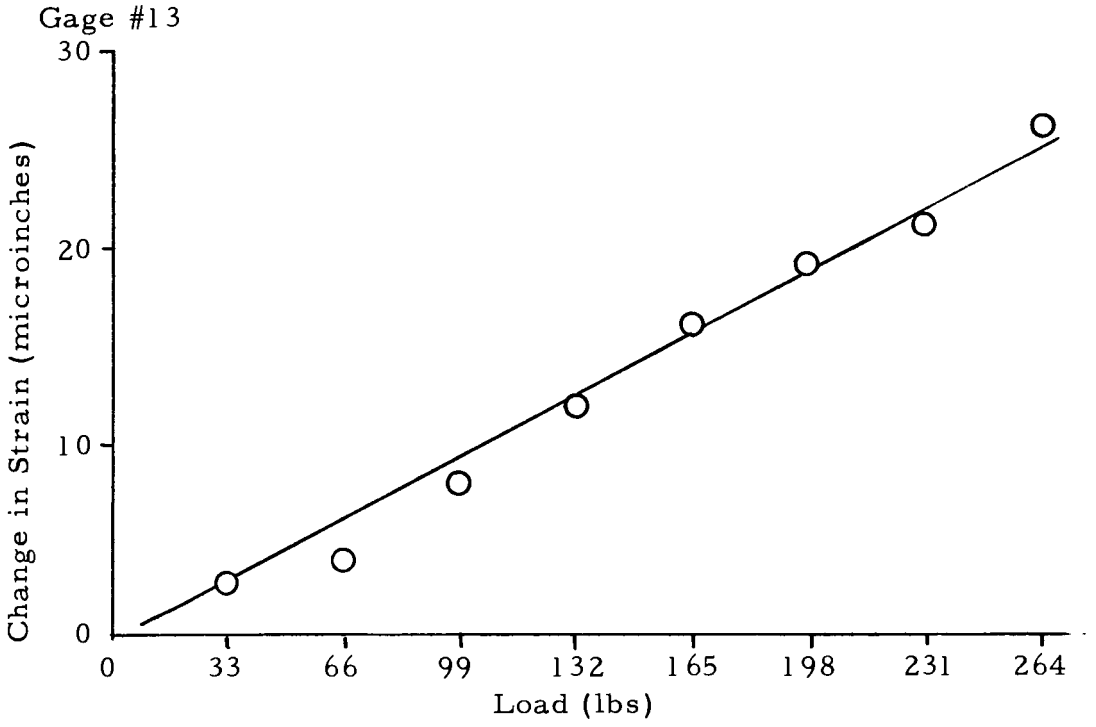

Load (lbs)	Gage Readings
0	18906
33	18909
66	18910
99	18914
132	18918
165	18922
198	18925
231	18927
264	18932

Figure 22. Load versus Strain.

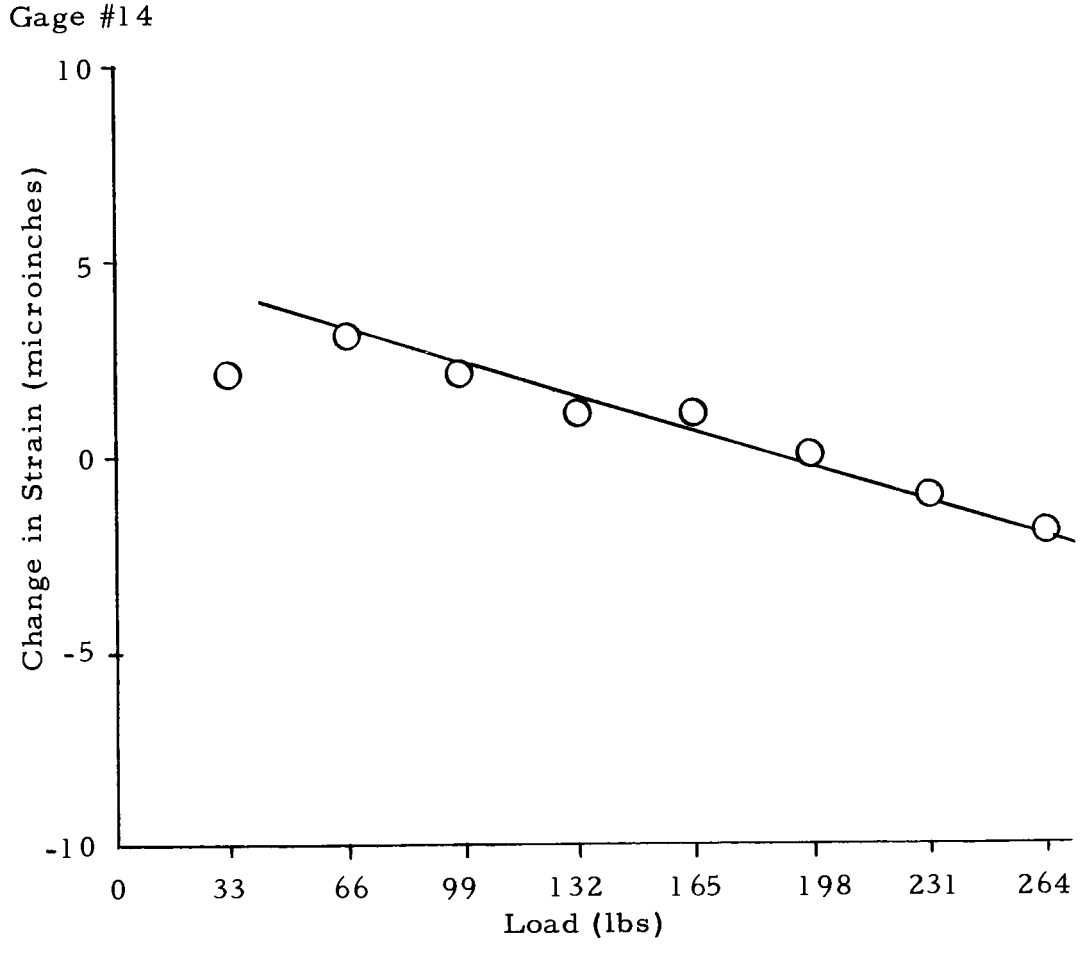

Load (lbs)	Gage Readings
0	16649
33	16651
66	16652
99	16651
132	16650
165	16650
198	16649
231	16648
264	16647

Figure 23. Load versus Strain.

Gage #15

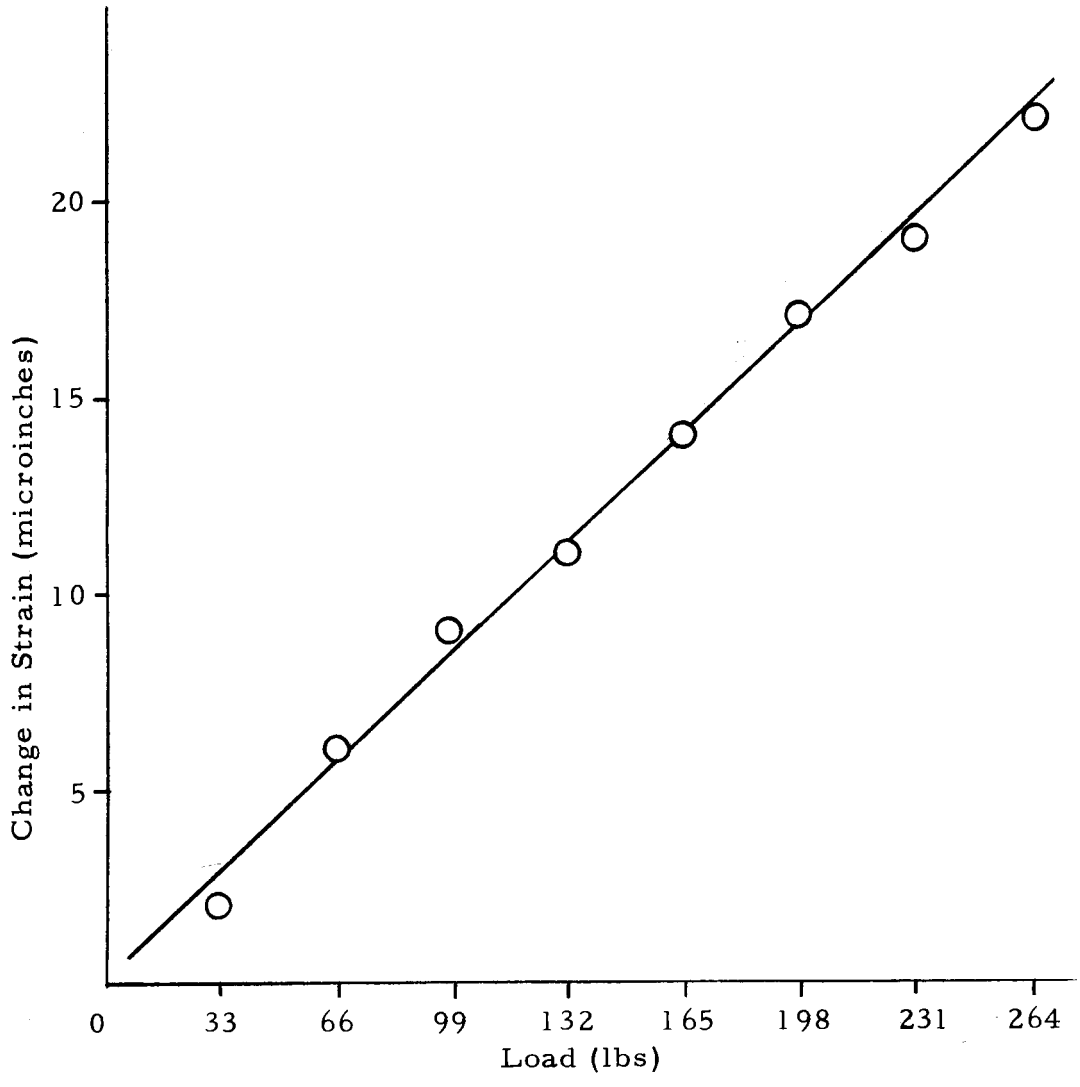

Load (lbs)	Gage Readings
0	15550
33	15552
66	15556
99	15559
132	15561
165	15564
198	15567
231	15569
264	15572

Figure 24. Load versus Strain.

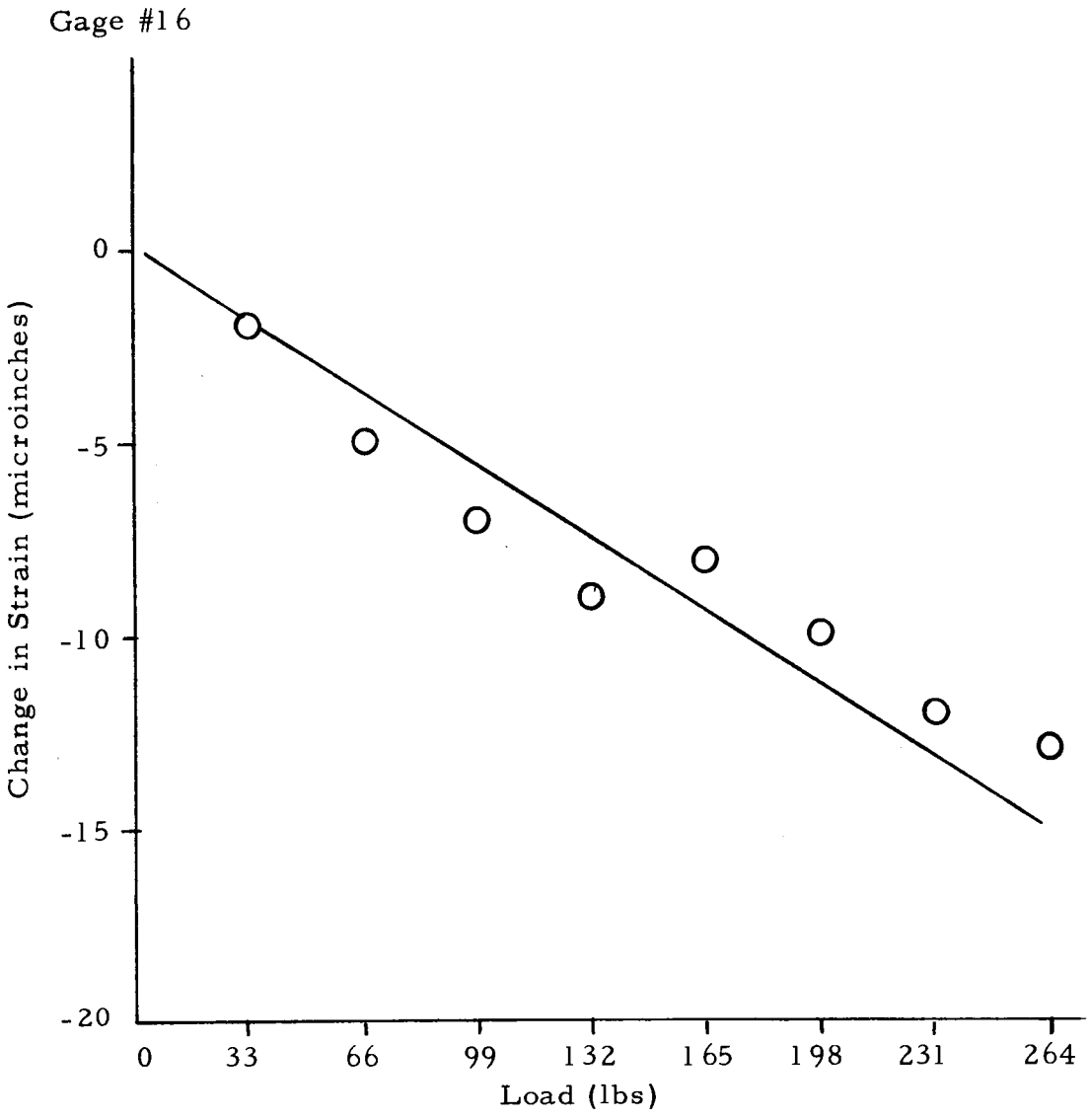

Load (lbs)	Gage Readings
0	19090
33	19088
66	19085
99	19083
132	19081
165	19082
198	19080
231	19078
264	19077

Figure 25. Load versus Strain.

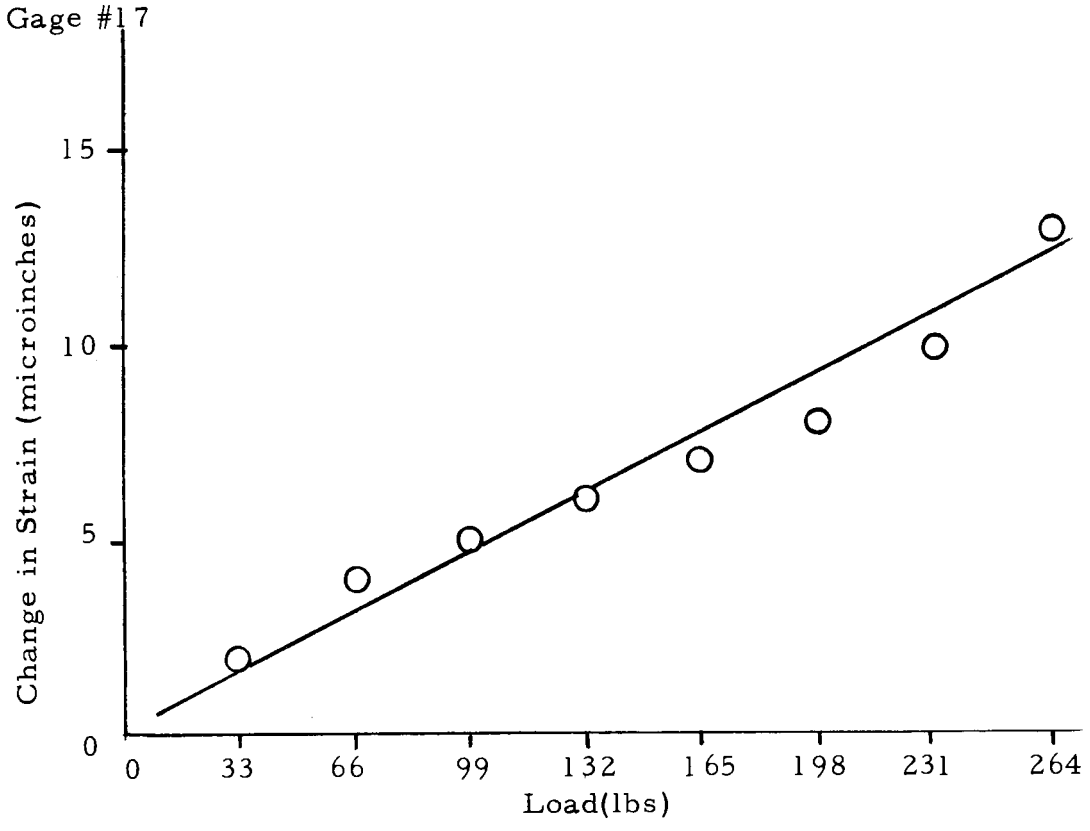

Load (lbs)	Gage Readings
0	15462
33	15464
66	15466
99	15467
132	15468
165	15469
198	15470
231	15472
264	15475

Figure 26. Load versus Strain.

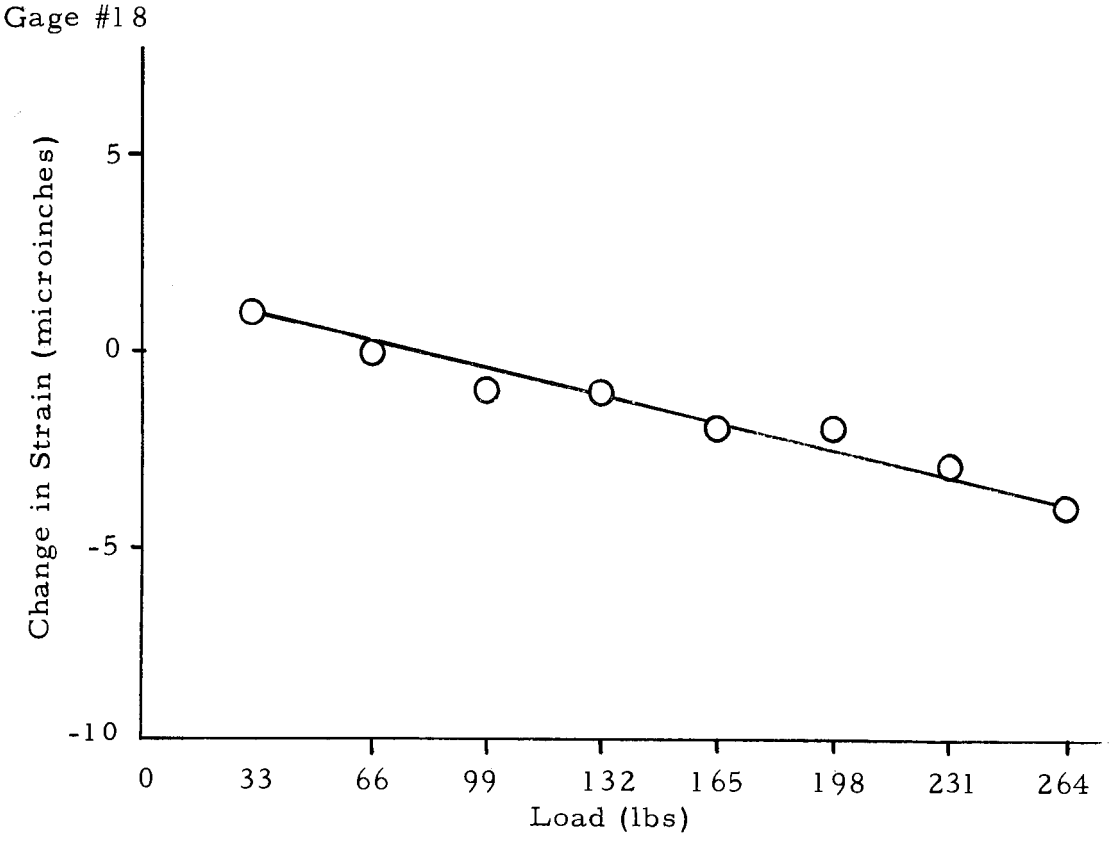

Load (lbs)	Gage Readings
0	16101
33	16102
66	16101
99	16100
132	16100
165	16099
198	16098
231	16098
264	16097

Figure 27. Load versus Strain.

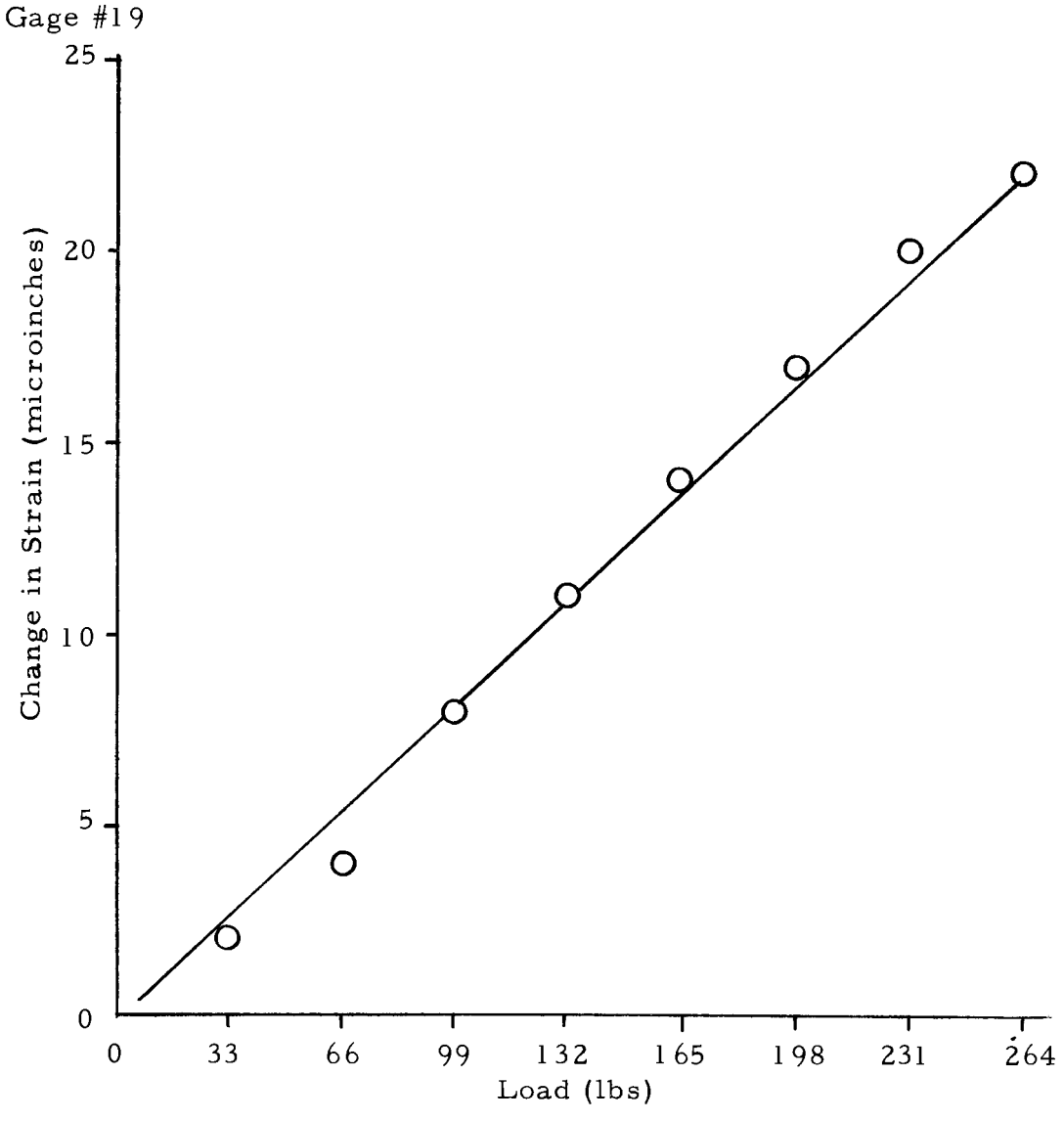

Load (lbs)	Gage Readings
0	17307
33	17309
66	17311
99	17315
132	17318
165	17321
198	17324
231	17327
264	17329

Figure 28. Load versus Strain.

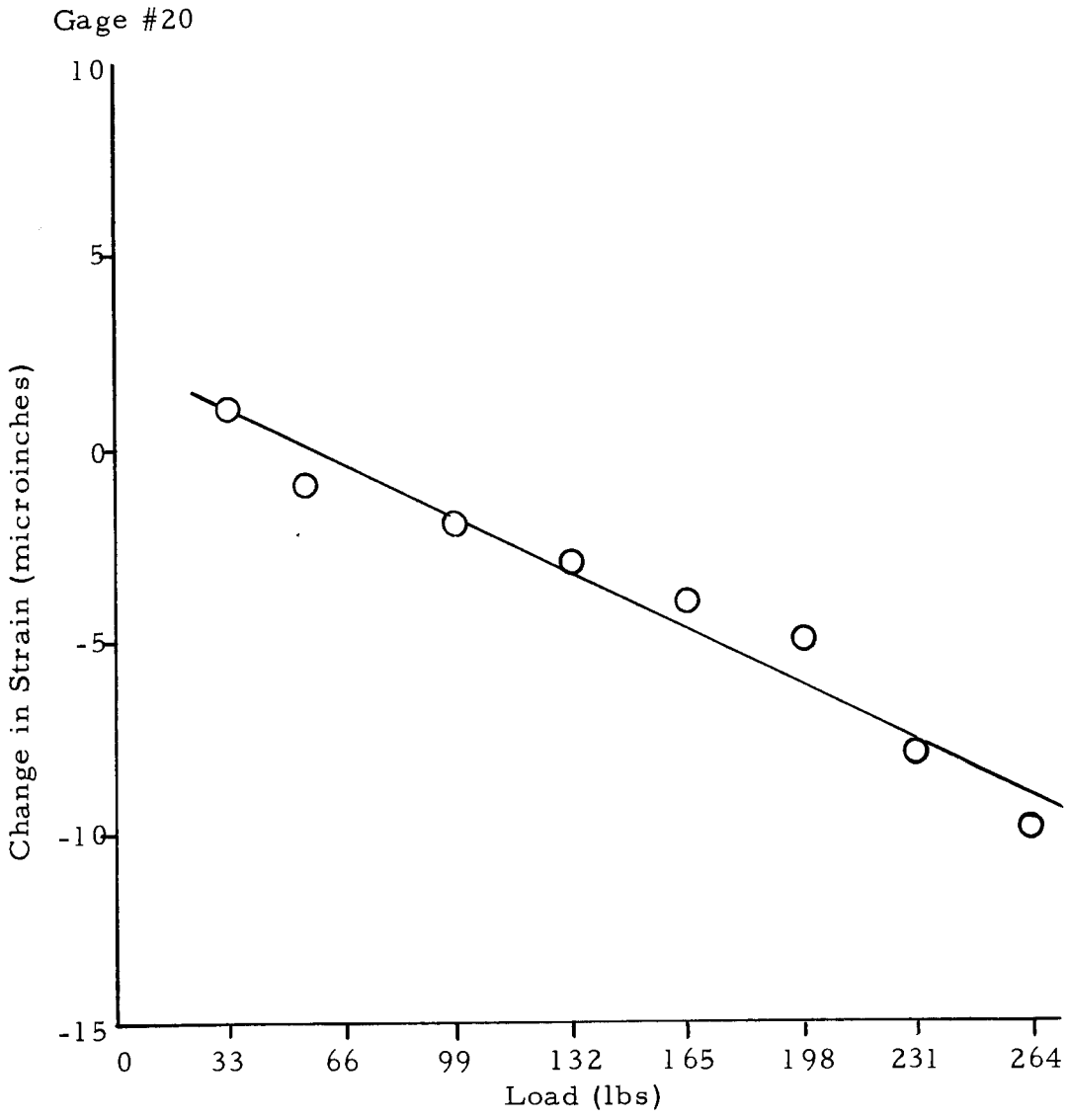

Load (lbs)	Gage Readings
0	14533
33	14534
66	14532
99	14531
132	14530
165	14529
198	14528
231	14525
264	14523

Figure 29. Load versus Strain.

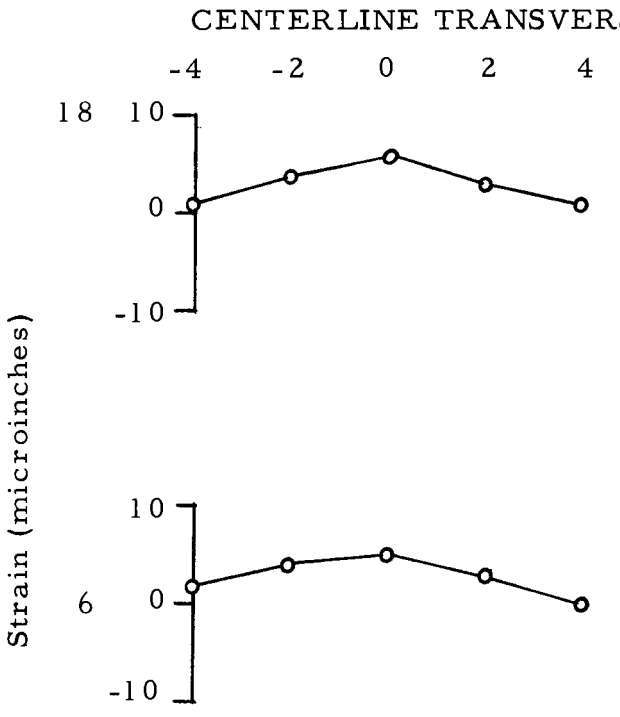

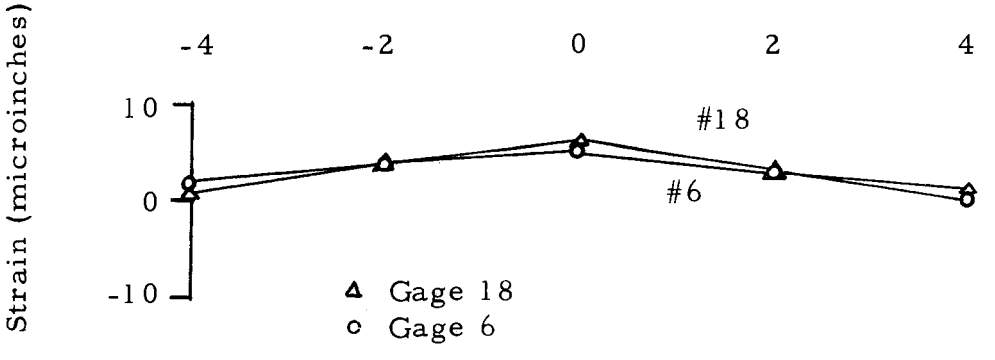

Figure 30. Comparison Between Centerline Gages of Skewed (#6) and Normal (#18) Joints When Loaded on Centerline.

3. Sample Computations

Skewed Joint Solid Slab

Equation 1) $$\epsilon_L = \frac{\sigma_L}{E} - \frac{\mu\ \sigma_T}{E}$$

Equation 2) $$\epsilon_T = \frac{\sigma_T}{E} - \frac{\mu\ \sigma_L}{E}$$

Equation 3) $$\sigma_{tensile} = \frac{\sigma_L + \sigma_T}{2}$$

Solving Equations 1 and 2 will provide values for σ_L and σ_T which will, when substituted in Equation 3, produce the tensile stress for the point in question

Gages 1 and 2

position -6

1) $11(3.5) = \sigma_L - 0.15\,\sigma_T$

2) $-2(3.5) = \sigma_T - 0.15\,\sigma_L$

1) $38.5 = \sigma_L - 0.15\,(-7 + 0.15\,\sigma_L)$

$$.977\ \sigma_L = 38.7 - 1.05 \qquad \sigma_L = \frac{37.65}{.977} = 38.5 \text{ psi}$$

$$\sigma_t = \frac{38.5 + (-1.24)}{2} = 18.6 \text{ psi}$$

position -4

1) $16(3.5) = \sigma_L - 0.15\,\sigma_T$

2) $-2(3.5) = \sigma_T - 0.15\,\sigma_L$

1) $56 = \sigma_L - 0.15(-7 + 0.15\ \sigma_L)$

$$.977\ \sigma_L = 56 - 1.05$$

$$\sigma_L = \frac{54.95}{.977} = 56$$

$$\sigma_T = -7 + 0.15(56)$$

$$= -7 + 8.4 = 1.4 \qquad \sigma_t = \frac{56 + 1.4}{2}$$

$$= \frac{57.4}{2} = 28.6 \text{ psi}$$

Gages 1 and 2

position -2

1) $16(3.5) = \sigma_L - .15\ \sigma_T$

2) $-7(3.5) = \sigma_T - .15\ \sigma_L$

1) $56 = \sigma_L - .15(-24.5 - .15\ \sigma_L)$

$$.977\ \sigma_L = 56 - 3.67$$

$$\sigma_L = \frac{52.3}{.977} = 53.5 \qquad \sigma_T = -24.5 + .15(53.5) = -16.5$$

$$\sigma_t = \frac{53.5 - 16.5}{2} = \frac{37}{2} = 18.5 \text{ psi}$$

position "O"

1) $18(3.5) = \sigma_L - 0.15\ \sigma_T$

2) $-6(3.5) = \sigma_T - 0.15\ \sigma_L$

1) $63 = \sigma_L - 0.15(-21 + 0.15\ \sigma_L)$

$$.977\ \sigma_L = 63 - 3.15$$

$$\sigma_L = \frac{59.88}{.977} = 61 \qquad \sigma_T = -21 + .15(61) = -11.9 \text{ psi}$$

$$\sigma_t = \frac{61 - 11.9}{2} = \frac{49.1}{2} = 24.6 \text{ psi}$$

position +2

1) $18(3.5) = \sigma_L - 0.15\ \sigma_T$

2) $-10(3.5) = \sigma_T - 0.15\ \sigma_L$

1) $63 = \sigma_L - 0.15(-35 + 0.15\ \sigma_L)$

$$.977\sigma_L = 63 - 5.25 = 57.7$$

$$\sigma_L = \frac{57.7}{.977} = 59 \qquad \sigma_T = -35 + .15(59) = -26.2$$

$$\sigma_t = \frac{59 - 26.2}{2} = \frac{32.8}{2} = 16.4 \text{ psi}$$

Gages 1 and 2

position +4

1) $13(3.5) = \sigma_L - 0.15\sigma_L$

2) $-11(3.5) = \sigma_T - 0.15\sigma_L$

1) $45.5 = \sigma_L - 0.15(-38.5 + 0.15\sigma_L)$

$$.977\ \sigma_L = 45.5 - 5.76 = 39.26$$

$$\sigma_L = \frac{39.26}{.977} = 40.2 \qquad \sigma_T = -38.5 + 0.15(40.2) = -32.5$$

$$\sigma_t = \frac{40.2 - 32.5}{2} = \frac{7.7}{2} = 3.8 \text{ psi}$$

Gages 3 and 4

position -6

1) $10(3.5) = \sigma_L - .15\,\sigma_T$

2) $-8(3.5) = \sigma_T - .15\,\sigma_L$

1) $35 = \sigma_L - .15(-28 + .15\,\sigma_L)$

$$.977\,\sigma_L = 35 - 4.20$$

$$\sigma_L = \frac{31.8}{.977} = 32.5 \qquad \sigma_T = -28 + .15(32.5) = -23.1$$

$$\sigma_t = \frac{32.5 - 23.1}{2} = \frac{9.4}{2} = 4.7 \text{ psi}$$

position -4

1) $16(3.5) = \sigma_L - .15\,\sigma_T$

2) $-7(3.5) = \sigma_T + .15\,\sigma_L$

1) $56 = \sigma_L - .15(-24.5 + 15\,\sigma_L)$

$$.977\,\sigma_L = 56 - 3.66$$

$$\sigma_L = \frac{52.34}{.977} = 53.5 \qquad \sigma_T = -24.5 + .15(53.5) = -16.5$$

$$\sigma_t = \frac{53.5 - 16.5}{2} = \frac{37}{2} = 18.5 \text{ psi}$$

Gages 3 and 4

position -2

1) $17(3.5) = \sigma_L - .15\,\sigma_T$

2) $-3(3.5) = \sigma_T - .15\,\sigma_L$

1) $59.5 = \sigma_L - .15(-10.5 + .15\,\sigma_L)$

$$.977\sigma_L = 59.5 - 1.56$$

$$\sigma_L = \frac{58}{.977} = 58 \quad \sigma_T = -10.5 + .15\,(61.5) = -1.8$$

$$\sigma_t = \frac{58 - 1.8}{2} = \frac{56.2}{2} = 28.1 \text{ psi}$$

position "O"

1) $19(3.5) = \sigma_L - .15\,\sigma_T$

2) $-3(3.5) = \sigma_T - .15\,\sigma_L$

1) $66.5 = \sigma_L - .15(-10.5 + .15\,\sigma_L)$

$$.977\sigma_L = 66.5 - 1.56$$

$$\sigma_L = \frac{65}{.977} = 66.4 \quad \sigma_T = -10.5 - .15(66.4) = 0 - .5$$

$$\sigma_t = \frac{70 + 5}{2} = 34.7 \text{ psi}$$

position + 2

1) $17\,(3.5) = \sigma_L - .15\,\sigma_T$

2) $-7(3.5) = \sigma_T - .15\,\sigma_L$

1) $59.5 = \sigma_L - .15(-24.5 + .15\,\sigma_L)$

$$.977\,\sigma_L = 59.5 - 3.66 = 55.9$$

$$\sigma_L = \frac{55.9}{.977} = 58 \quad \sigma_T = -24.5 + .15(58) = -15.8$$

$$\sigma_t = \frac{58 - 15.8}{2} = \frac{42.2}{2} = 21.1 \text{ psi}$$

Gages 3 and 4

position -6

1) $21(3.5) = \sigma_L - .15\sigma_T$

2) $-4(3.5) = \sigma_T - .15\sigma_L$

1) $73.5 = \sigma_L - .15(-14 + .15\sigma_L)$

$$.977\sigma_L = 73.5 - 2.10$$

$$\sigma_L = \frac{71.4}{.977} = 73 \quad \sigma_T = -14 + .15(77.5) = -3.1$$

$$\sigma_t = \frac{71.4 - 3.1}{2} = \frac{68.3}{2} = 34.1 \text{ psi}$$

position -4

1) $26(3.5) = \sigma_L - .15\sigma_T$

2) $-3(3.5) = \sigma_T - .15\sigma_L$

1) $91 = \sigma_L - .15(-10.5 + .15\sigma_L)$

$$.977\sigma_L = 91 - 1.55$$

$$\sigma_L = \frac{89.45}{.977} = 91.5 \quad \sigma_T = -10.5 + .15(94.6) = +3.2$$

$$\sigma_t = \frac{91.5 + 3.2}{2} = \frac{94.7}{2} = 47.3 \text{ psi}$$

position -2

1) $29(3.5) = \sigma_L - .15\sigma_T$

2) $0 = \sigma_T - .15\sigma_L$

1) $101.5 = \sigma_L - .15(.15\sigma_L)$

$$\sigma_L = \frac{101.5}{.977} = 104 \quad \sigma_T = 0 + .15(104) = 15.5$$

$$\sigma_t = \frac{119.5}{2} = 59.8 \text{ psi}$$

position "O"

1) $31(3.5) = \sigma_L - .15\sigma_T$

2) $1(3.5) = \sigma_T - .15\sigma_L$

1) $108.5 = \sigma_L - .15(3.5 + .15\sigma_L)$

$$.977\sigma_L = 108.5 + .452$$

$$\sigma_L = \frac{108.95}{.977} = 112 \quad \sigma_T = 3.5 + .15(112) = 20.3$$

$$\sigma_t = \frac{132.3}{2} = 66.1 \text{ psi}$$

Gages 3 and 4

position +4

1) $10(3.5) = \sigma_L - .15\sigma_T$

2) $-11(3.5) = \sigma_T - .15\sigma_L$

1) $35 = \sigma_L - .15(-38.5 + .15\sigma_L)$

$$.977\sigma_L = 35 - 5.75$$

$$\sigma_L = \frac{29.25}{.977} = 30 \quad \sigma_T = -38.5 + .15(91.8) = -34$$

$$\sigma_t = \frac{30 - 34}{2} = -2 \text{ psi}$$

Gages 5 and 6

position +4

1) $20(3.5) = \sigma_L - .15\sigma_T$

2) $-10(3.5) = \sigma_T - .15\sigma_L$

1) $70 = \sigma_L - .15(-35 + .15\sigma_L)$

$64.75 = .977\sigma_L \quad \sigma_L = 66.4 \quad \sigma_T = -35 + .15(66.4) = -25.1$

$$\sigma_t = \frac{66.4 - 25.1}{2} = \frac{41.3}{2} = 20.6 \text{ psi}$$

position +2

1) $21(3.5) = \sigma_L - .15\sigma_T$

2) $7(3.5) = \sigma_T - .15\sigma_L$

1) $73.5 = \sigma_L - .15(-24.5 + .15\sigma_L$

$70 = .977\sigma_L \quad \sigma_L = 71.6 \quad \sigma_T = -24.5 + .15(71.6) = -13.8$

$$\sigma_t = \frac{71.6 - 13.8}{2} = \frac{57.8}{2} = 28.9 \text{ psi}$$

position "O"

1) $24(3.5) = \sigma_L - .15\sigma_T$

2) $5(3.5) = \sigma_T - .15\sigma_L$

1) $84 = \sigma_L - .15(-17.5 + .15\sigma_L)$

$81.4 = .977\sigma_L \quad \sigma_L = 83 \quad \sigma_T = -17.5 + .15(83) = -5$

$$\sigma_t = \frac{83 - 5}{2} = \frac{78}{2} = 39 \text{ psi}$$

Gages 5 and 6

position -2

1) $28(3.5) = \sigma_L - .15\sigma_T$

2) $4(3.5) = \sigma_T - .15\sigma_L$

1) $98 = \sigma_L - .15(-14 + .15\sigma_L)$

$$97.9 = .977\sigma_L \qquad \sigma_L = 99 \qquad \sigma_T = -14 + .15(99) = +1$$

$$\sigma_t = \frac{99 + 1}{2} = 50 \text{ psi}$$

position -4

1) $24(3.5) = \sigma_L - .15\sigma_T$

2) $-3(3.5) = \sigma_T - .15\sigma_L$

1) $84 = \sigma_L - .15(-10.5 + .15\sigma_L)$

$$82.5 = .977\sigma_L \qquad \sigma_L = 84.5 \qquad \sigma_T = -10.5 + .15(84.5) = +2.2$$

$$\sigma_t = \frac{84.5 + 2.2}{2} = \frac{86.7}{2} = 43.3 \text{ psi}$$

position -6

1) $21(3.5) = \sigma_L - .15\sigma_T$

2) $-2(3.5) = \sigma_T - .15\sigma_L$

1) $73.5 = \sigma_L - .15(-7 + .15\sigma_L)$

$$72.5 = .977\sigma_L \qquad \sigma_L = 74 \qquad \sigma_T = -7 + .15(74) = +4$$

$$\sigma_t = \frac{74 + 4}{2} = \frac{78}{2} = 39 \text{ psi}$$

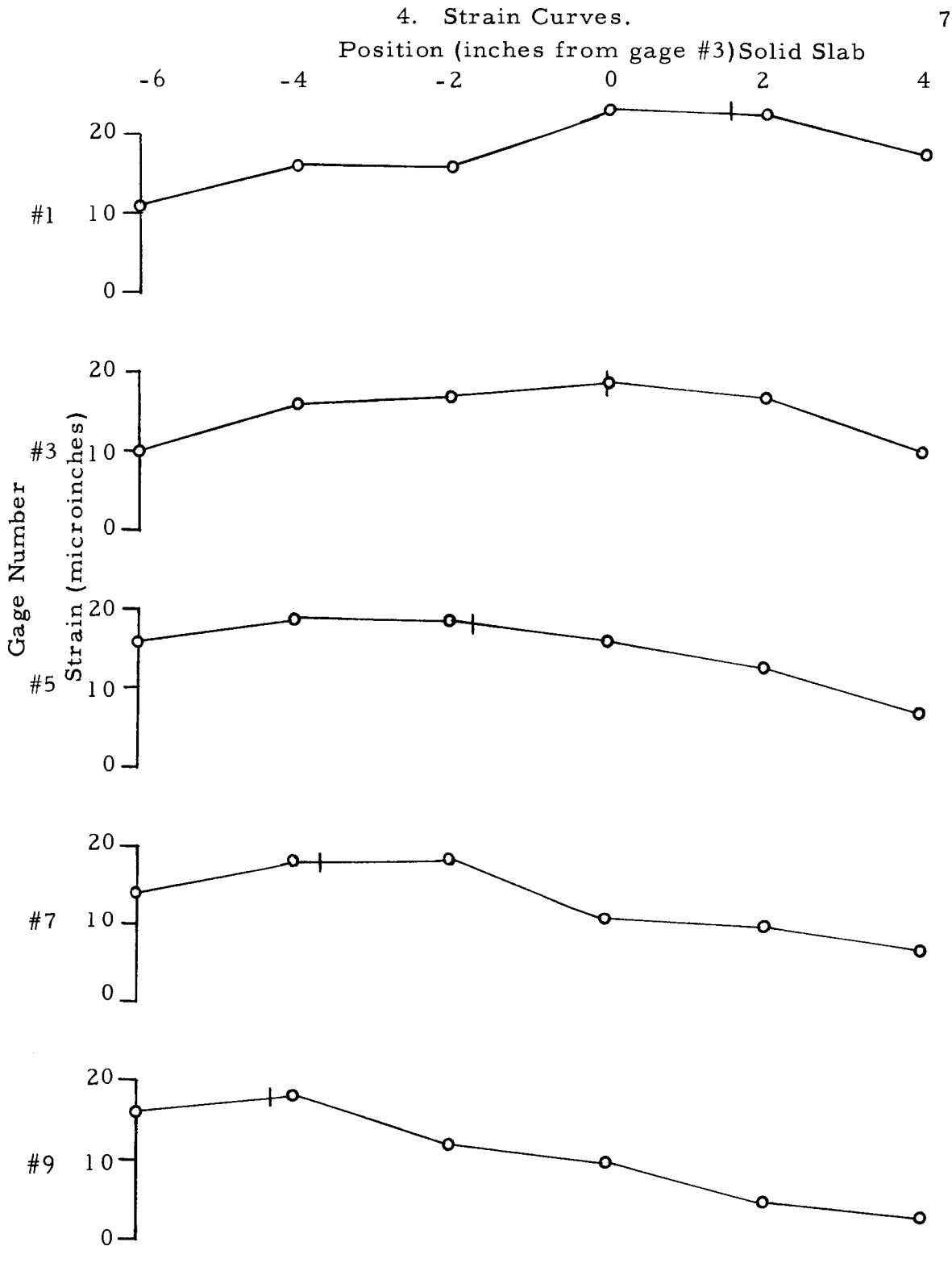

Figure 31. Longitudinal Strain Curve.

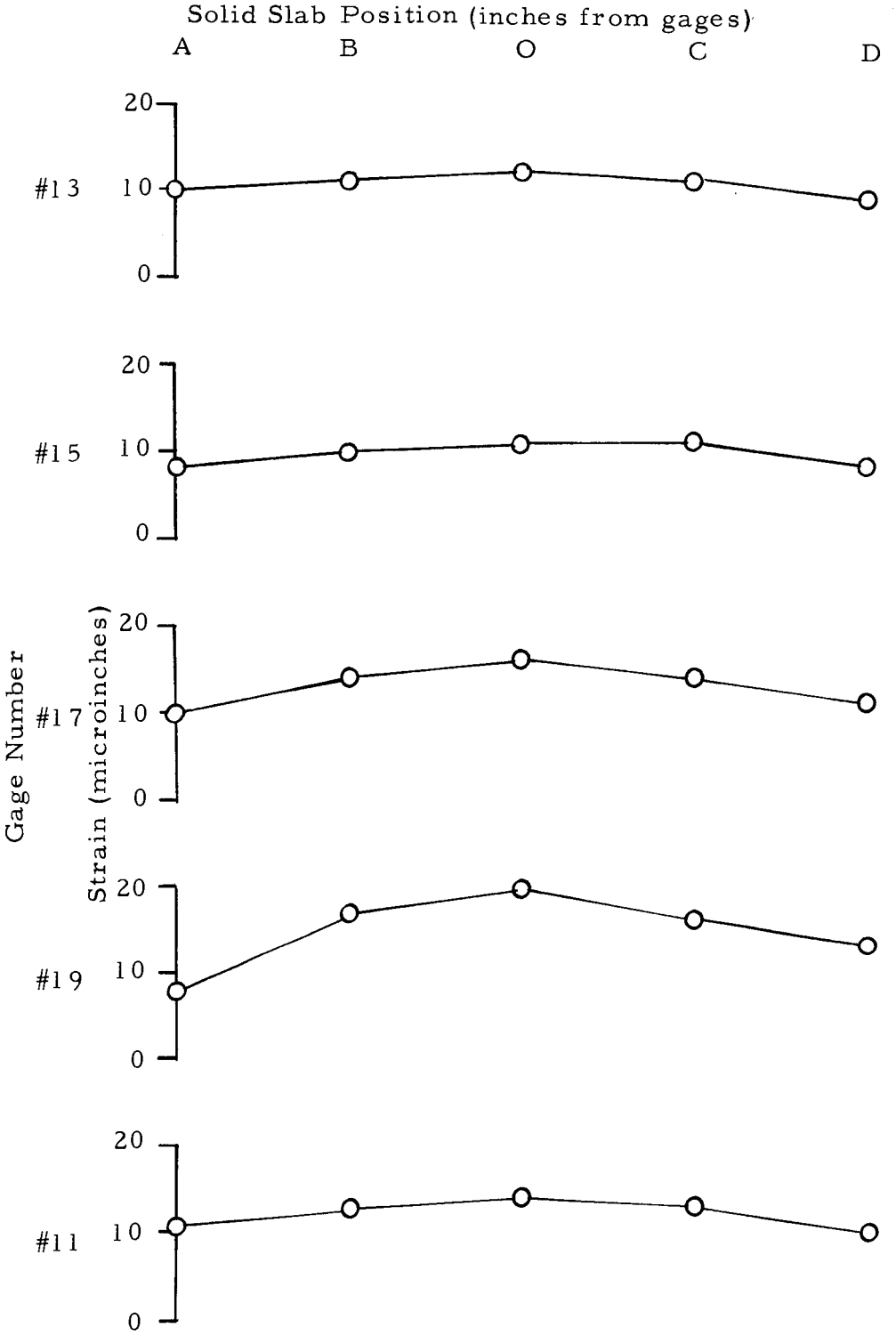

Figure 32. Longitudinal Strain Curve.

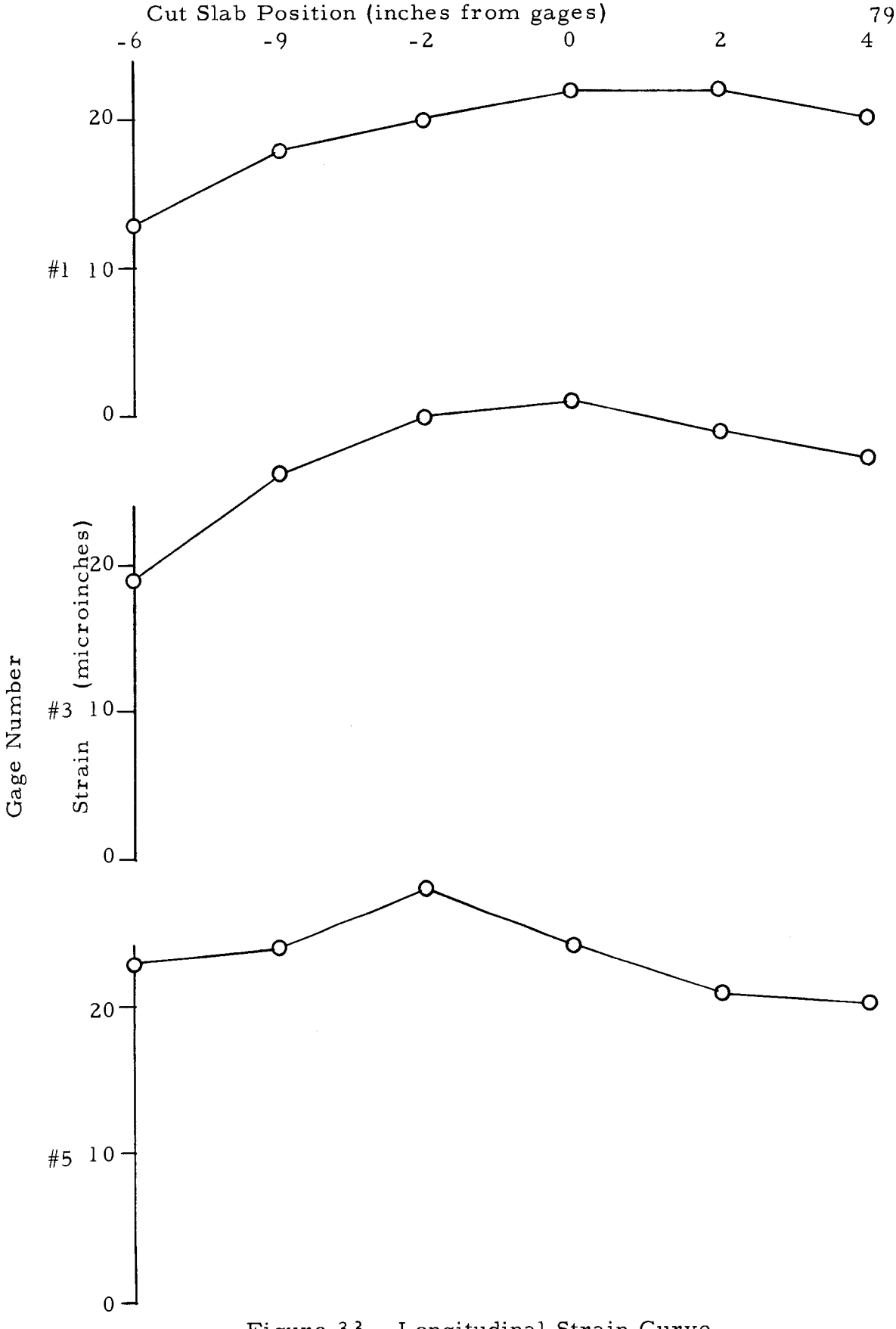

Figure 33. Longitudinal Strain Curve.

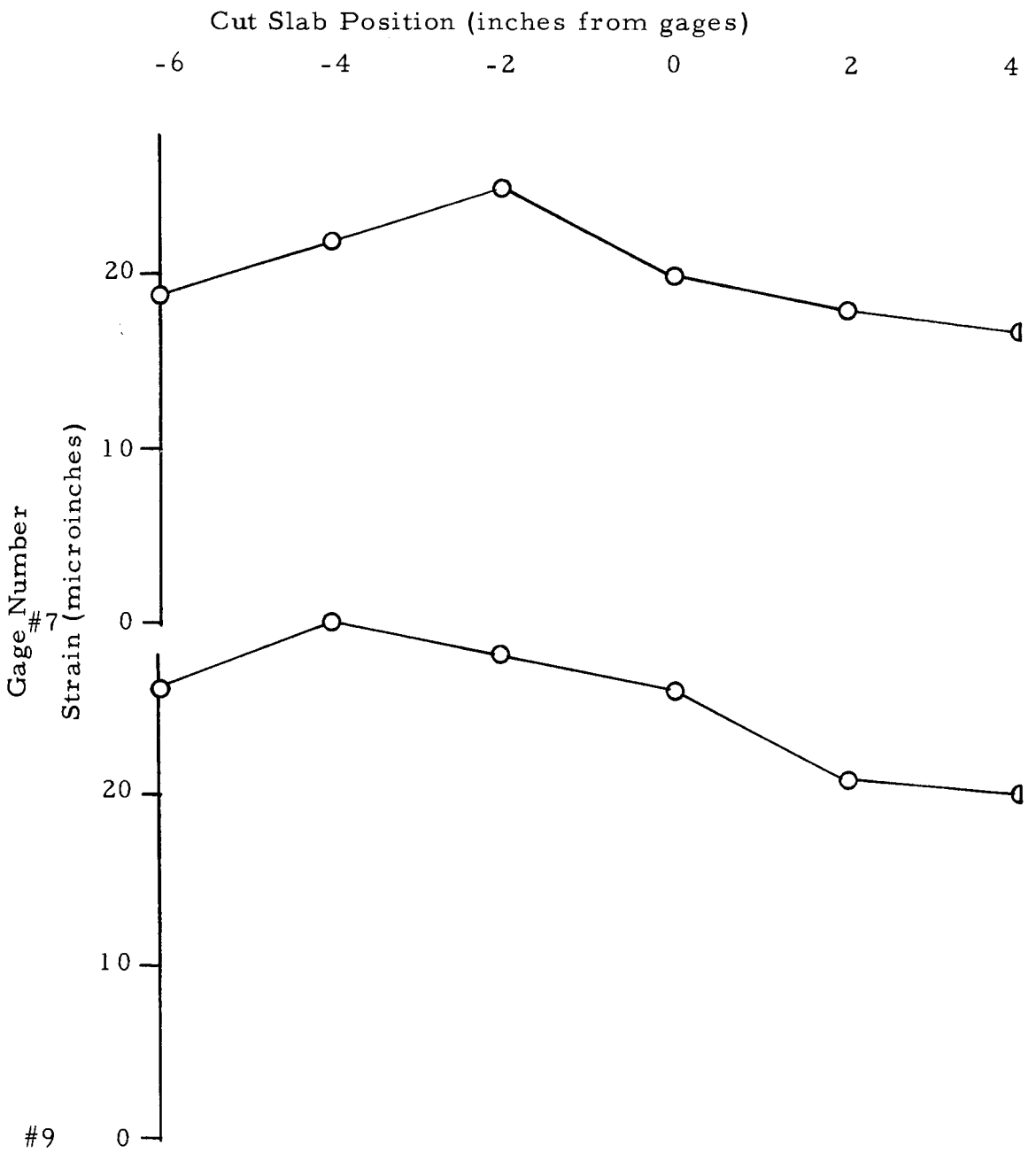

Figure 34. Longitudinal Strain Curve.

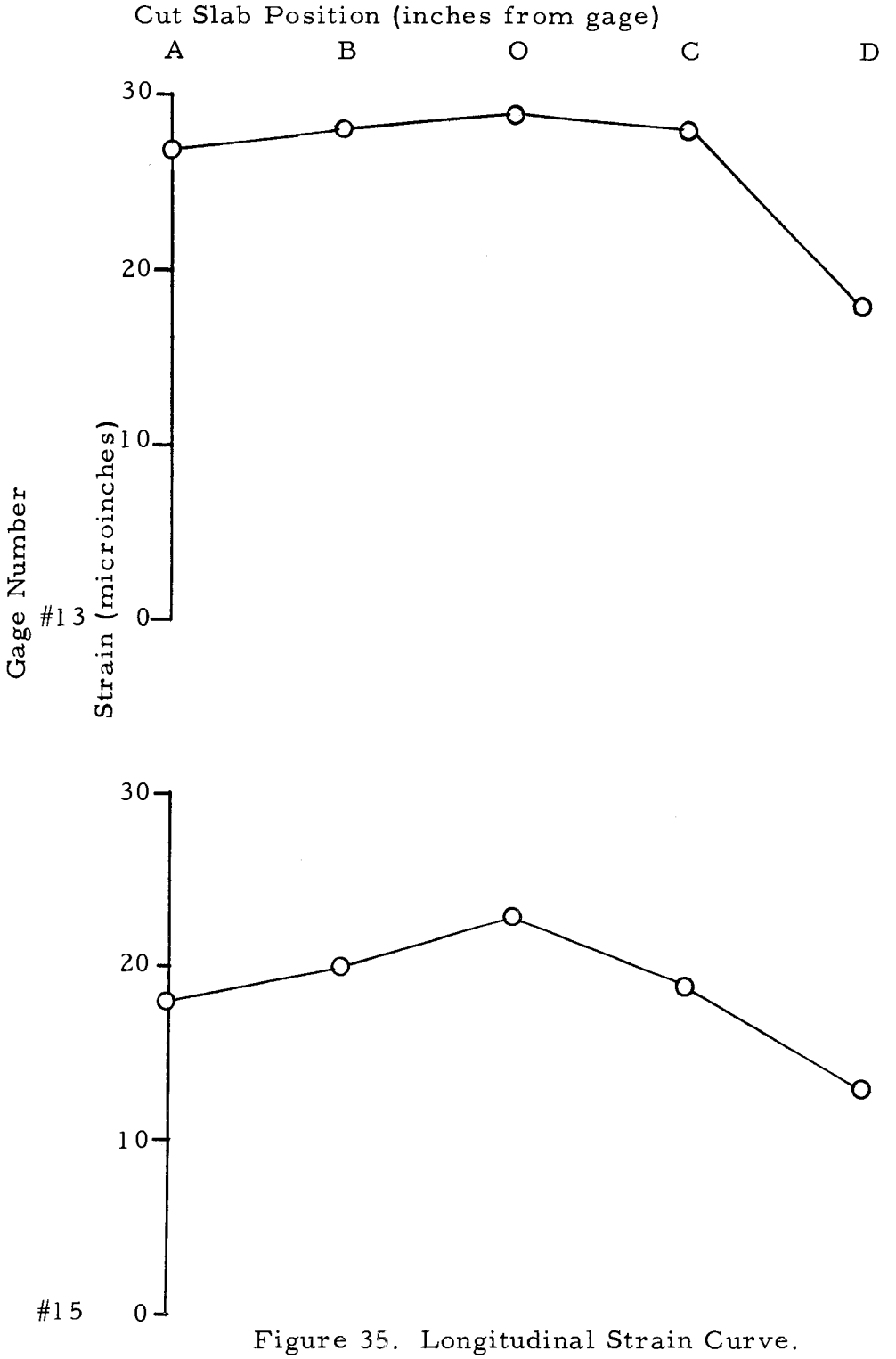

Figure 35. Longitudinal Strain Curve.

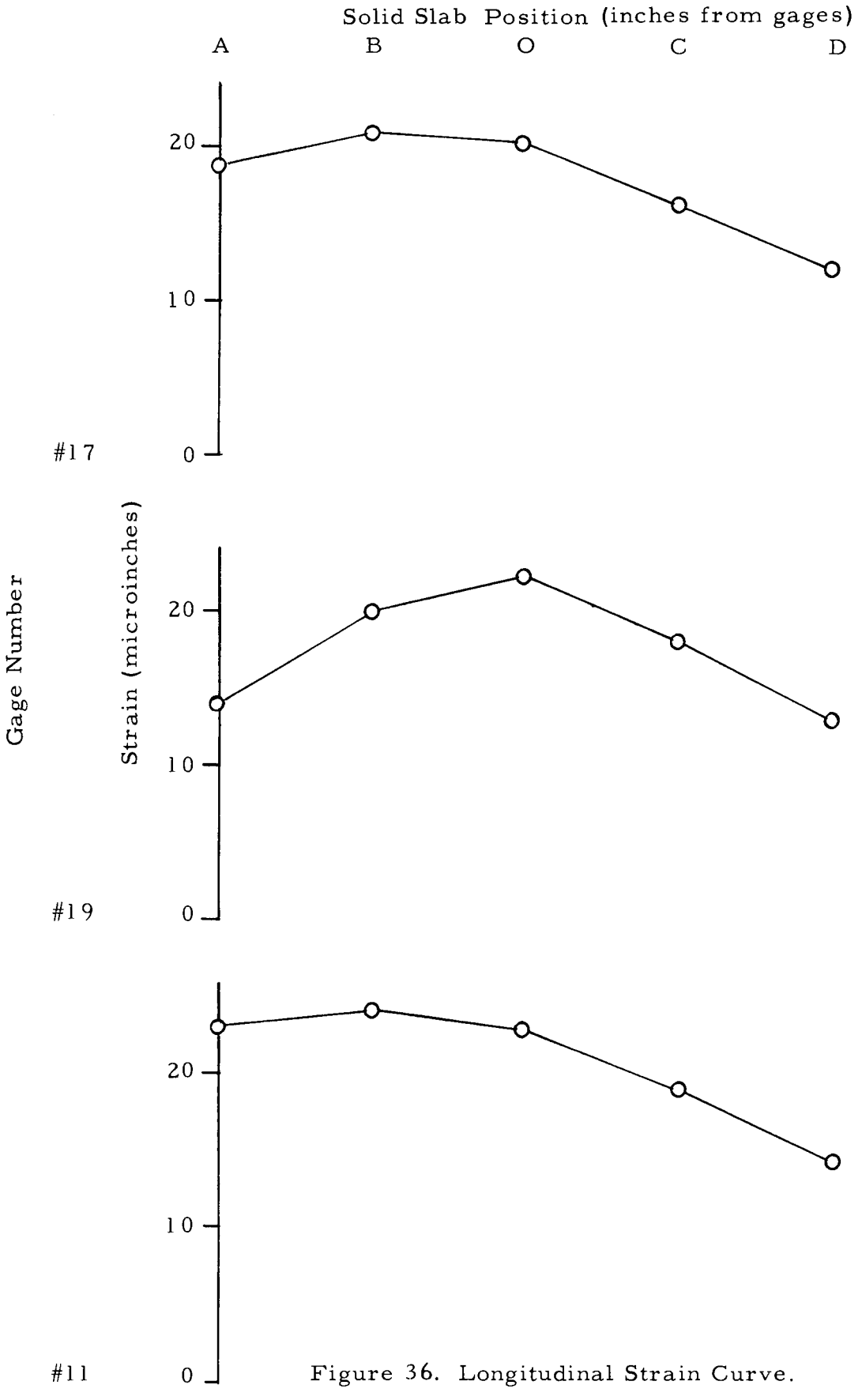

Figure 36. Longitudinal Strain Curve.

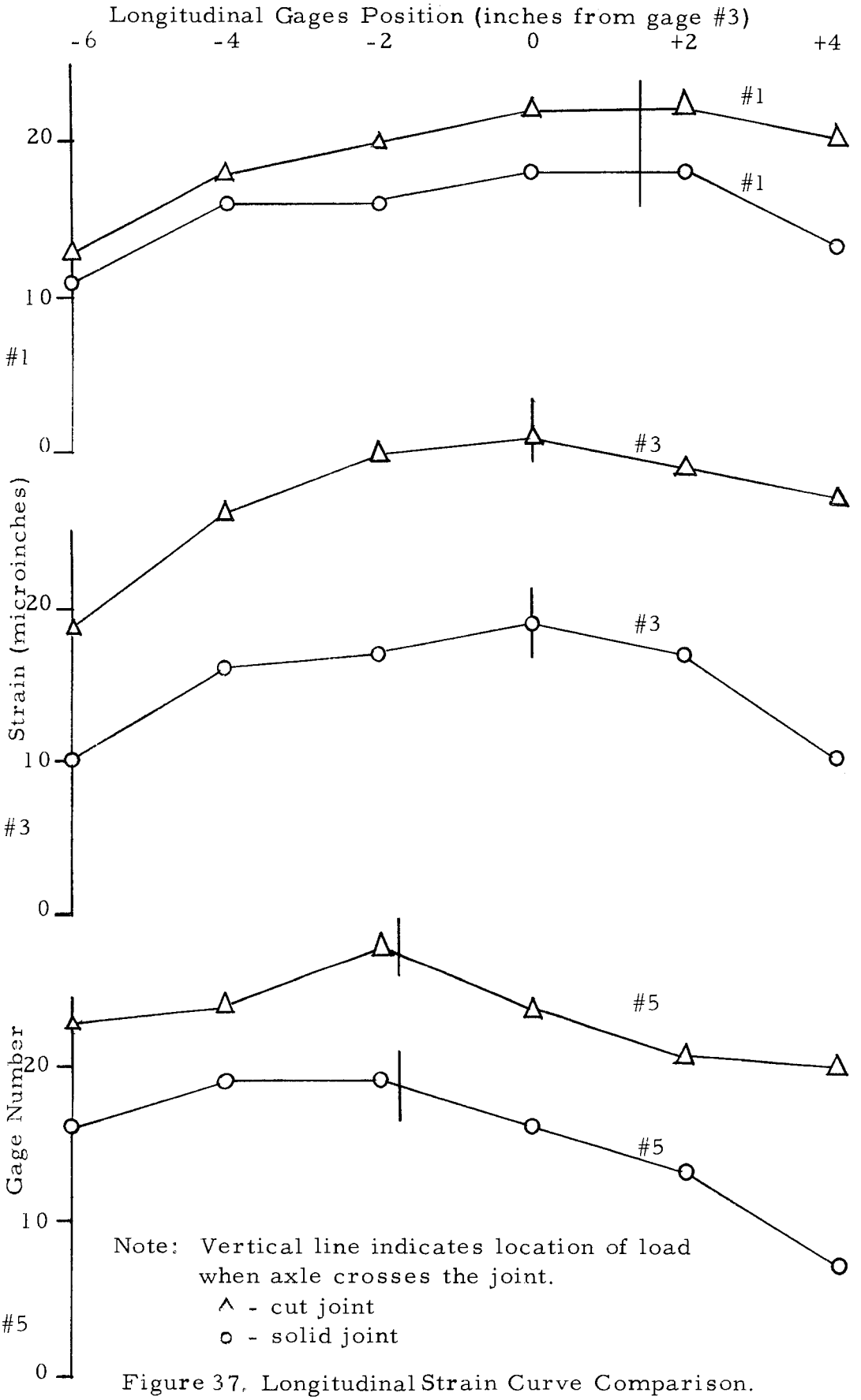

Note: Vertical line indicates location of load when axle crosses the joint.

^ - cut joint

o - solid joint

Figure 37. Longitudinal Strain Curve Comparison.

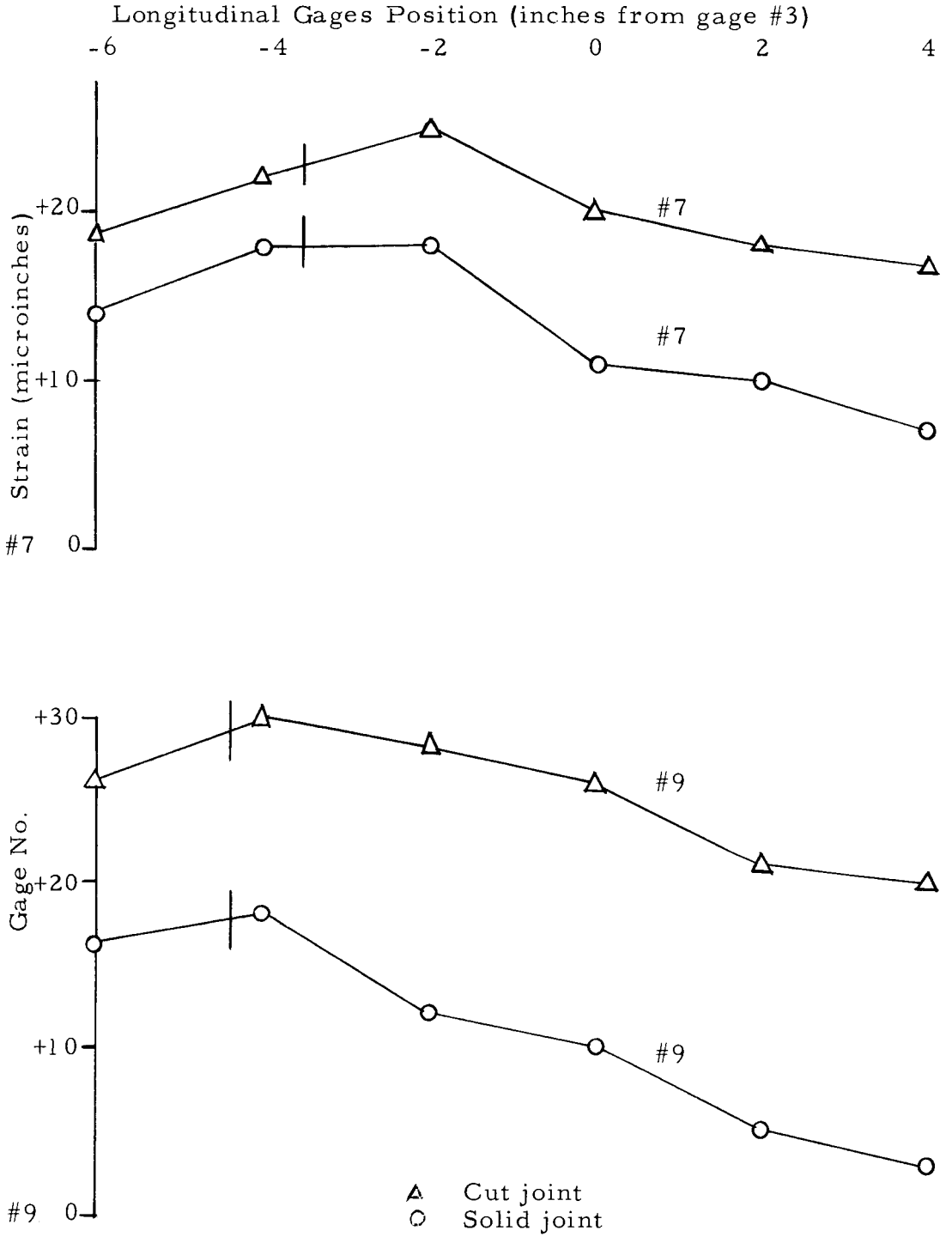

Figure 38. Longitudinal Strain Curve Comparison.

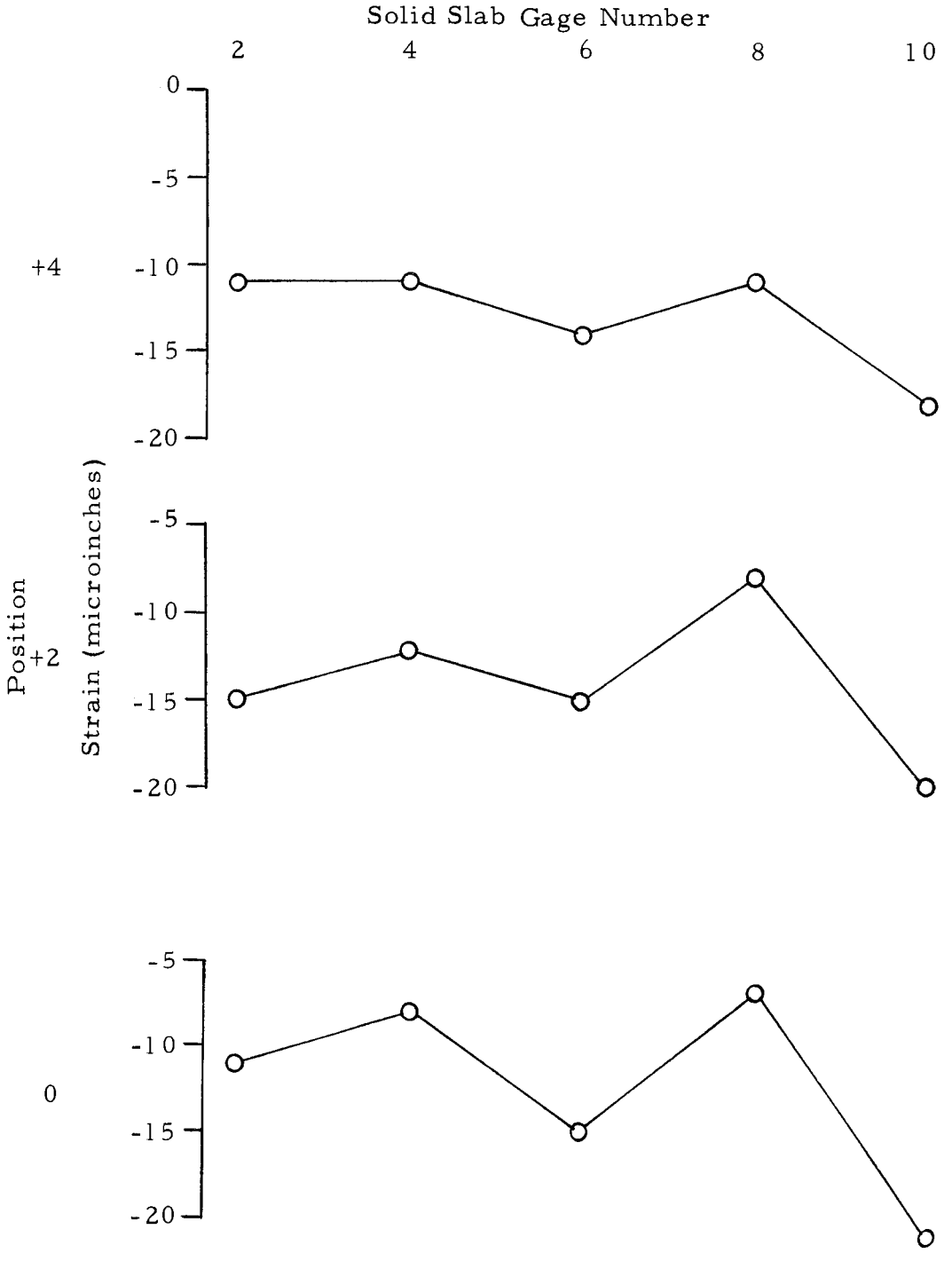

Figure 39. Transverse Strain Curve.

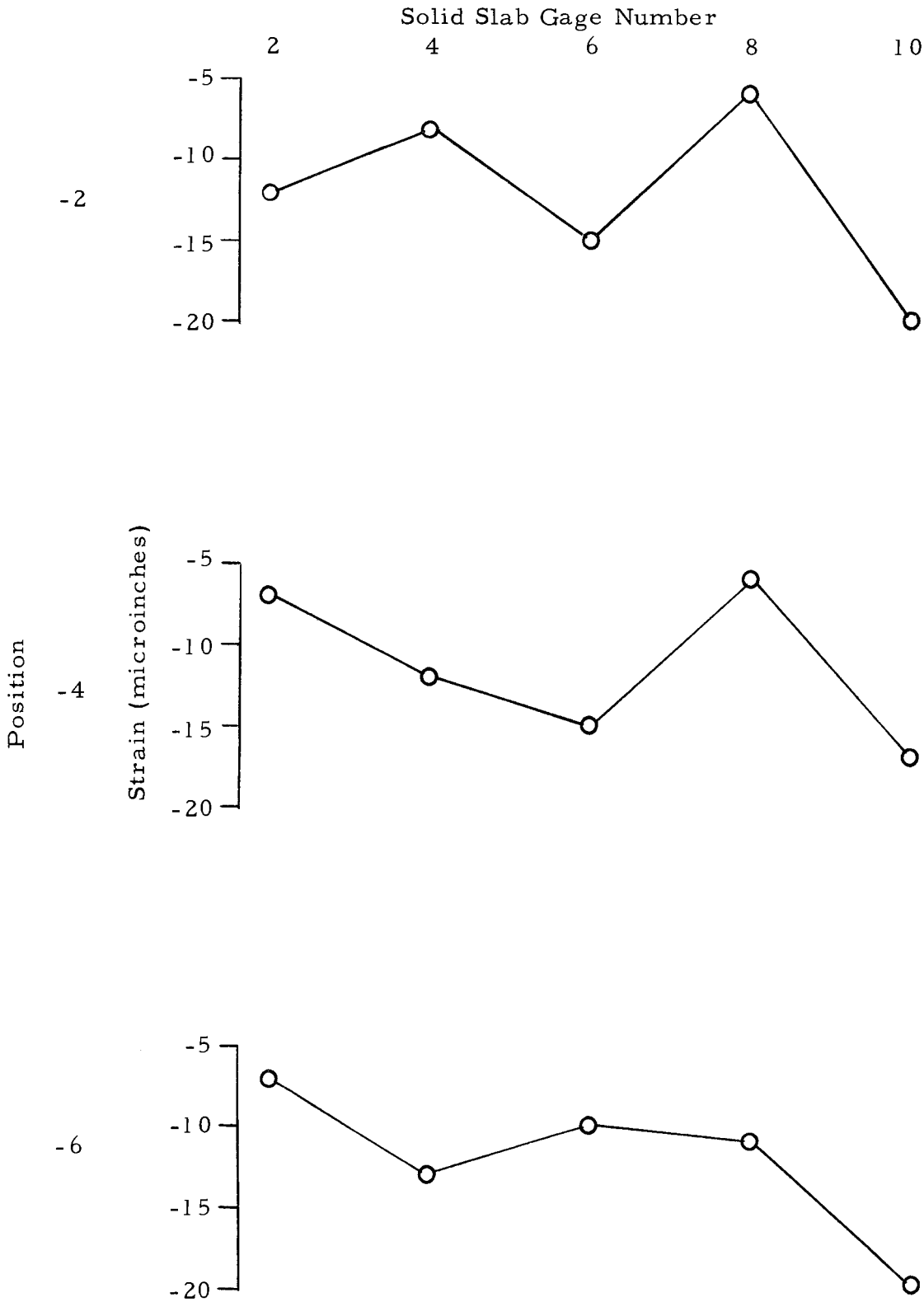

Figure 40. Transverse Strain Curve.

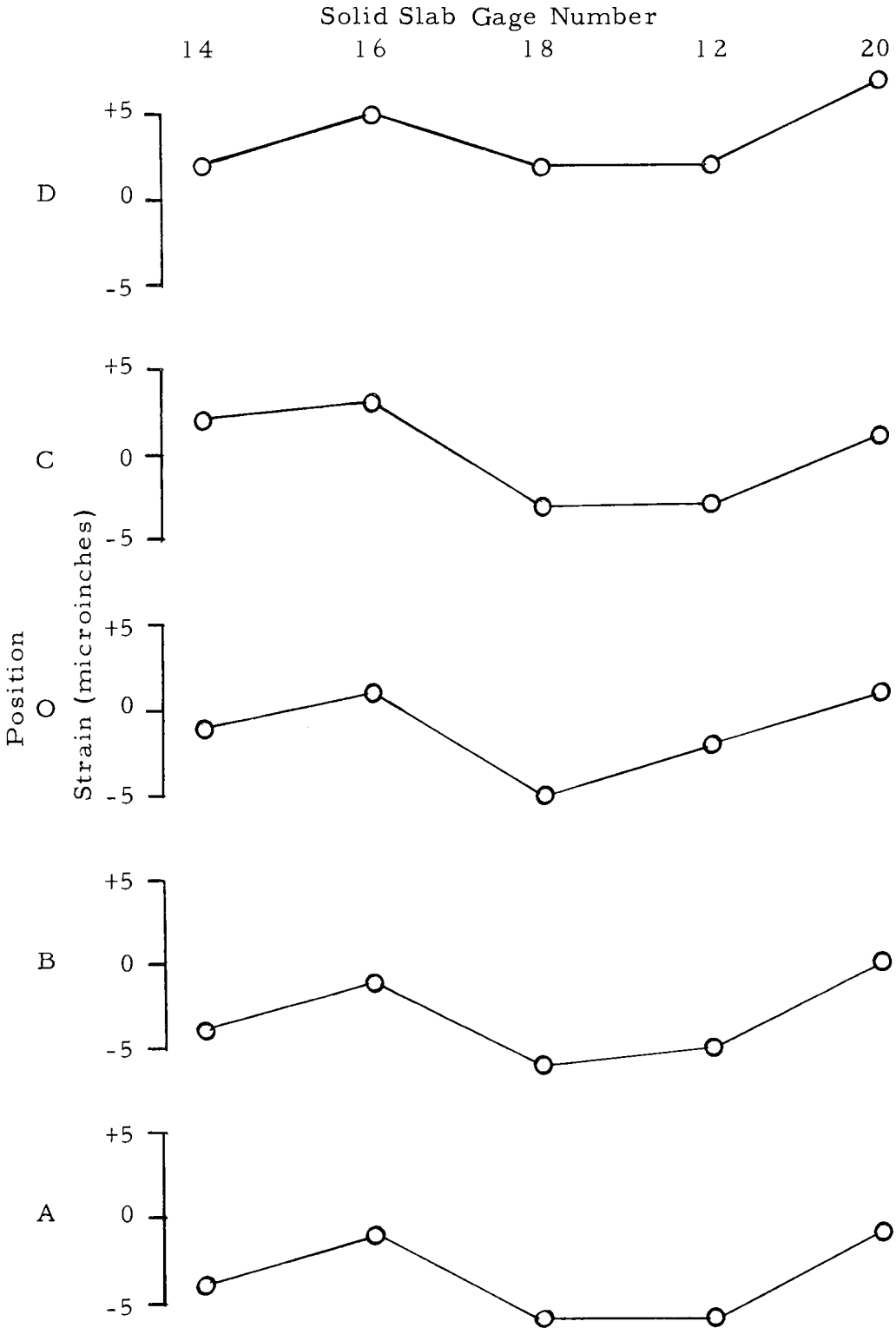

Figure 41. Transverse Strain Curve.

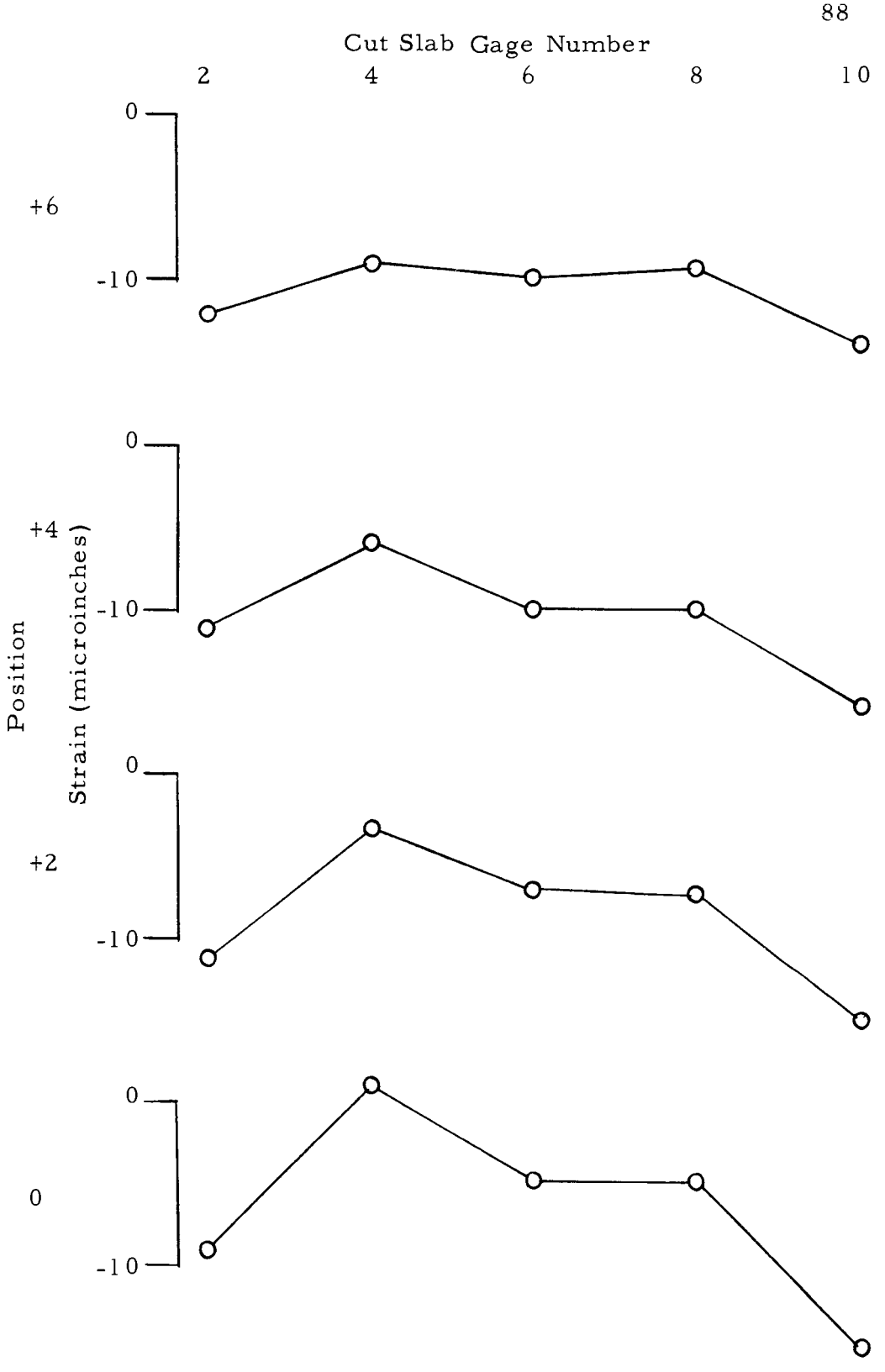

Figure 42. Transverse Strain Curve.

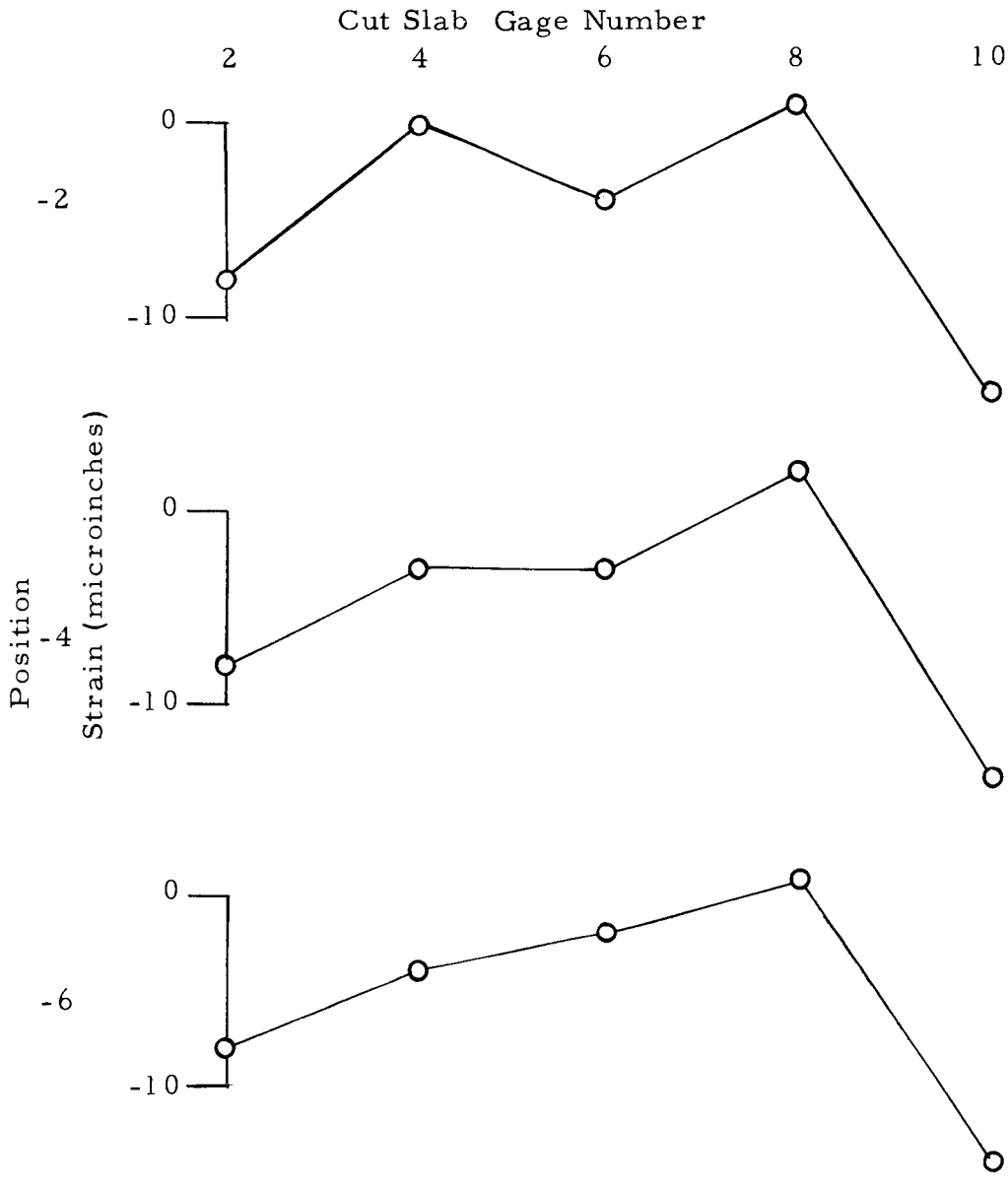

Figure 43. Transverse Strain Curve.

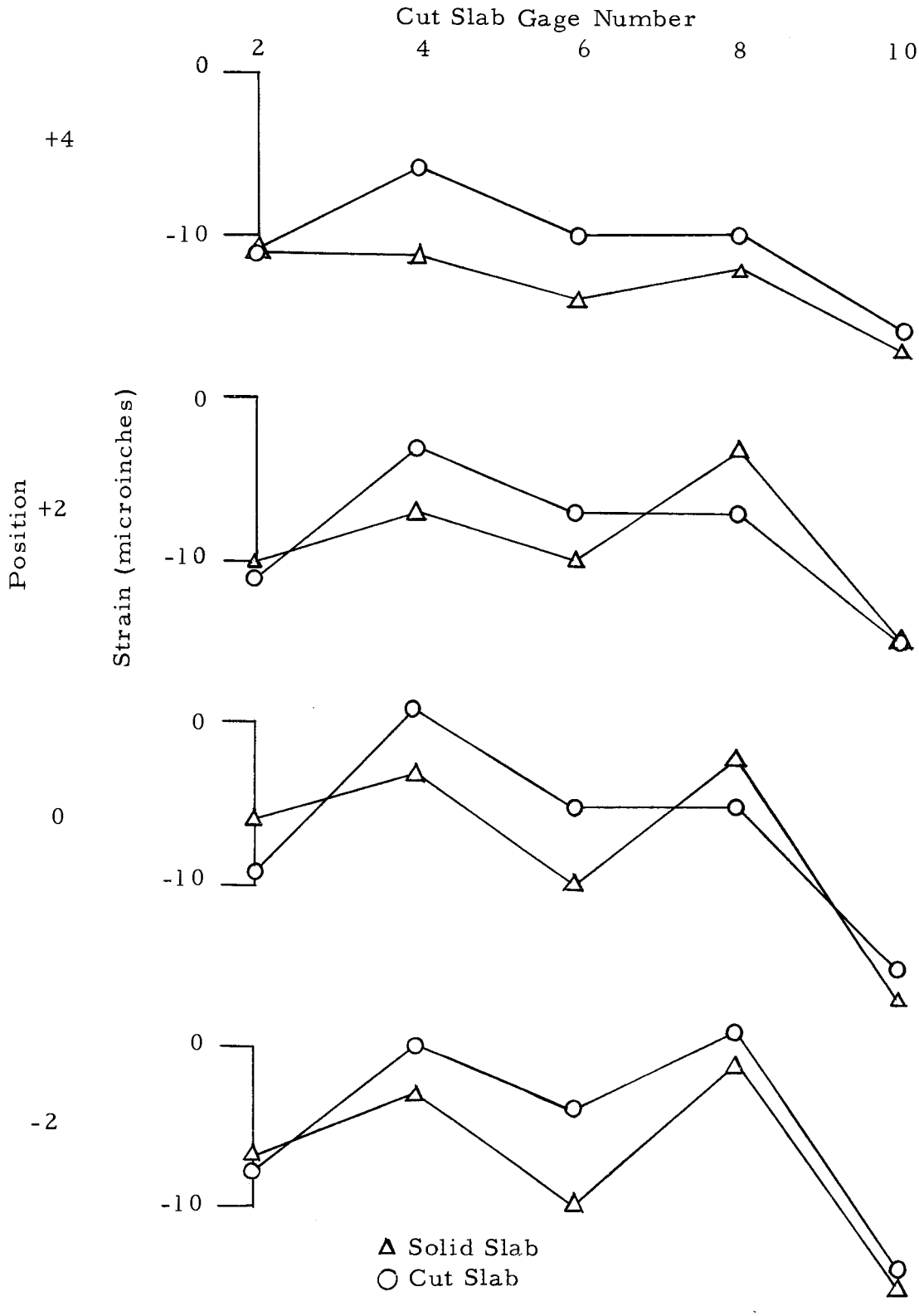

Figure 44. Transverse Strain Curve Comparison.

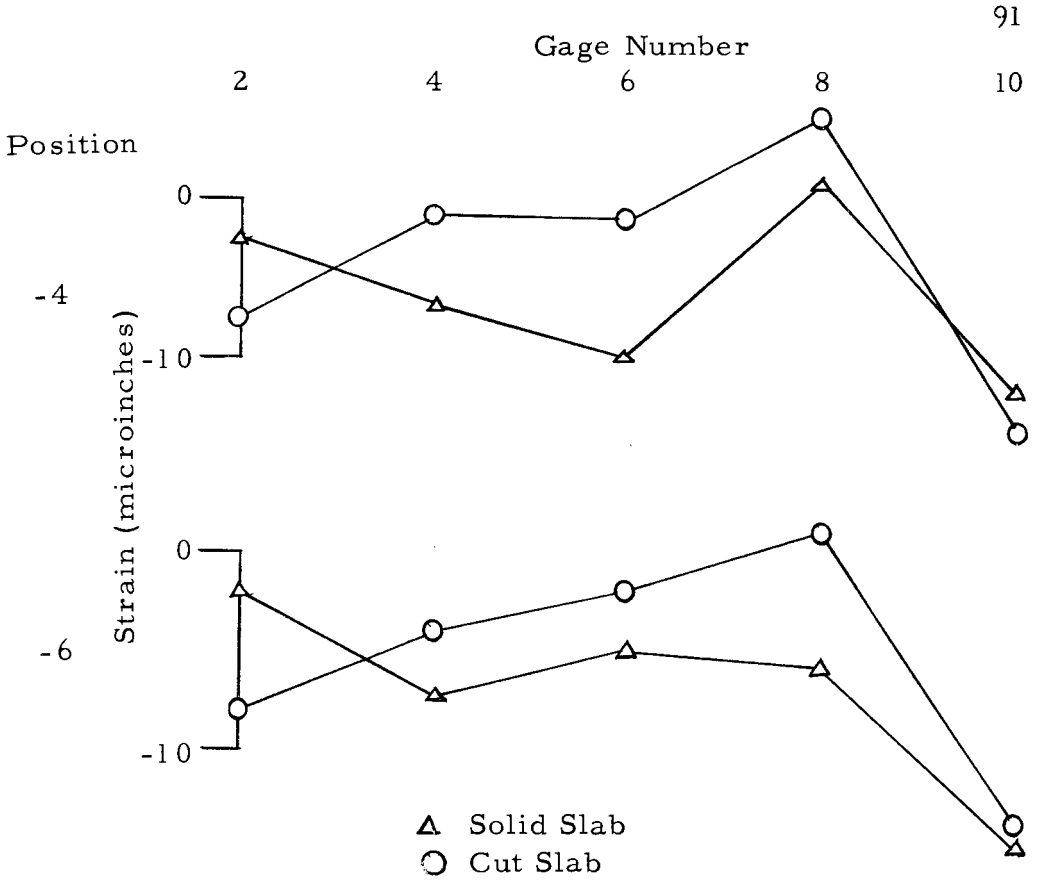

Figure 45. Transverse Strain Curve Comparison.

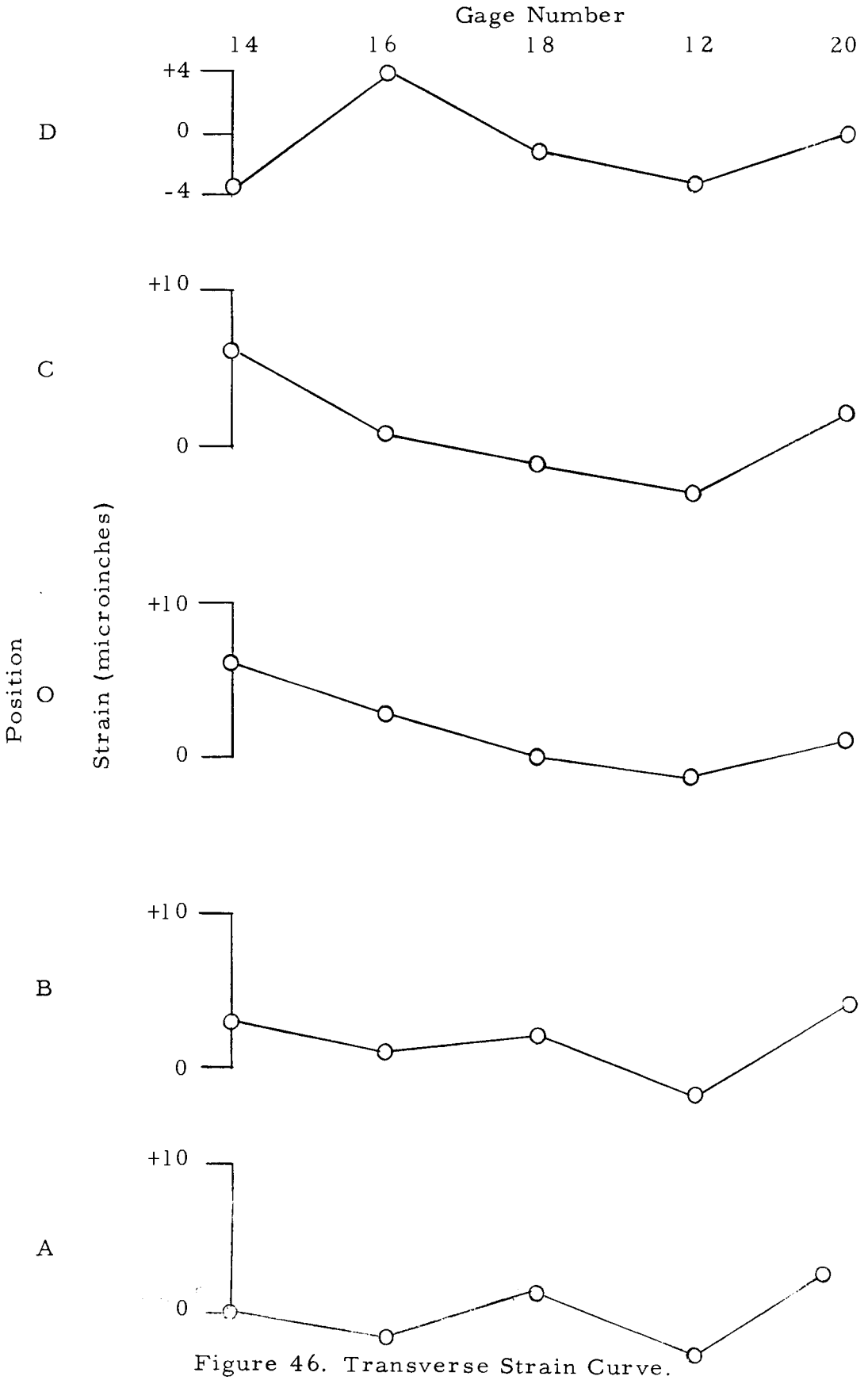

Figure 46. Transverse Strain Curve.